

การป้องกันน้ำท่วมเมืองที่มีสถานะเป็นนครโดยการยับยั้งกระบวนการเกิดออกซิเดชันของแร่ไฟไรต์  
ด้วยการสร้างเหล็กฟอสเฟตเคลือบผิว



นาย นิพนธ์ คงมาก

สถาบันวิทยบริการ

วิทยานิพนธ์นี้เป็นส่วนหนึ่งของการศึกษาตามหลักสูตรปริญญาวิทยาศาสตรมหาบัณฑิต

สาขาวิชาการจัดการสิ่งแวดล้อม (สหสาขาวิชา)

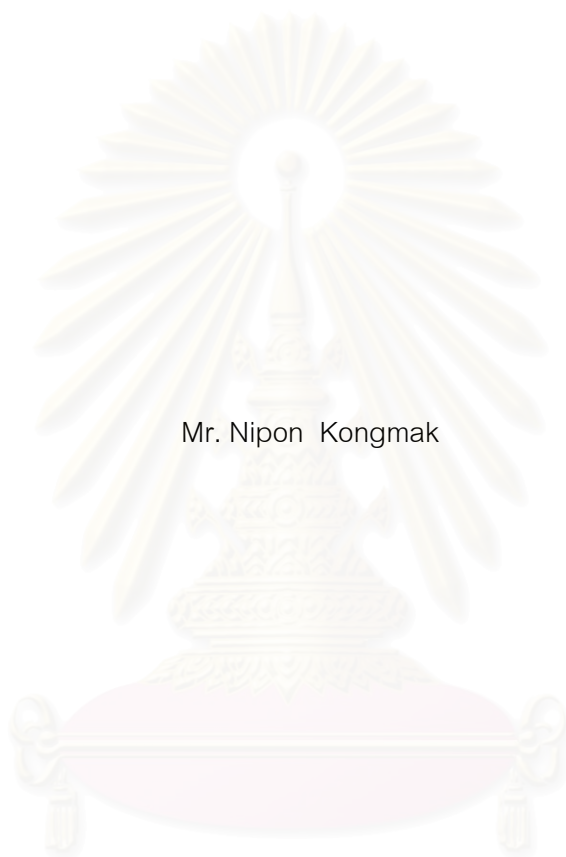
บัณฑิตวิทยาลัย จุฬาลงกรณ์มหาวิทยาลัย

ปีการศึกษา 2548

ISBN 974-17-5756-5

ลิขสิทธิ์ของจุฬาลงกรณ์มหาวิทยาลัย

ACID MINE DRAINAGE PREVENTION BY SUPPRESSION OF PYRITE OXIDATION WITH  
IRON-PHOSPHATE COATING ON PYRITE SURFACES



Mr. Nipon Kongmak

สถาบันวิทยบริการ

A Thesis Submitted in Partial Fulfillment of the Requirements  
For the Degree of Master of Science Program in Environmental Management (Inter-Department)

Graduate School

Chulalongkorn University

Academic Year 2005

ISBN 974-17-5756-5

Copyright of Chulalongkorn University

Thesis Title                      Acid mine drainage prevention by suppression of pyrite oxidation  
with iron-phosphate coating on pyrite surfaces

By                                      Mr. Nipon Kongmak

Field of study                      Environmental Management

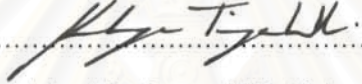
Thesis Advisor                      Chantra Tongcumpou, Ph.D.

Thesis Co-advisor                      Assistant Professor Chakkaphan Sutthirat, Ph.D.

---

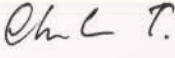
Accepted by the Graduate School, Chulalongkorn University in Partial

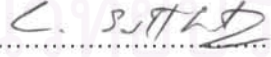
Fulfillment of the Requirements for the Master's Degree

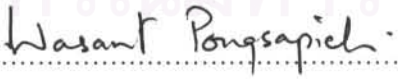
  
..... Dean of the Graduate School  
(Assistant Professor M.R. Kalaya Tingsabadh, Ph.D.)

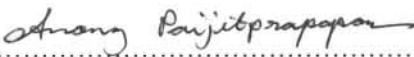
THESIS COMMITTEE

  
..... Chairman  
(Manaskorn Rachakornkij, Ph.D.)

  
..... Thesis Advisor  
(Chantra Tongcumpou, Ph.D.)

  
..... Thesis Co-advisor  
(Assistant Professor Chakkaphan Sutthirat, Ph.D.)

  
..... Member  
(Associate Professor Wasant Pongsapich, Ph.D.)

  
..... Member  
(Anong Paijitprapapon, M.Sc.)

นิพนธ์ กงมาก : การป้องกันน้ำขุมเหมืองที่มีสถานะเป็นกรดโดยการยับยั้งกระบวนการเกิดออกซิเดชันของแร่ไพไรต์ด้วยการสร้างเปลือกฟอสเฟตเคลือบผิว. (ACID MINE DRAINAGE PREVENTION BY SUPPRESSION OF PYRITE OXIDATION WITH IRON-PHOSPHATE COATING ON PYRITE SURFACES) อ. ที่ปรึกษา : อ. ดร. จันทรา ทองคำเถา, อ.ที่ปรึกษาร่วม : ผศ. ดร. จักรพันธ์ สุทธิรัตน์ 97 หน้า. ISBN 974-17-5756-5.

การศึกษานี้มีวัตถุประสงค์เพื่อศึกษาความเป็นไปได้ และกำหนดสภาวะที่เหมาะสมในการสร้างเปลือกฟอสเฟตเคลือบผิวของแร่ไพไรต์เพื่อยับยั้งกระบวนการเกิดออกซิเดชันของแร่ไพไรต์ และป้องกันการเกิดสภาพของน้ำขุมเหมืองเป็นกรด ตัวอย่างแร่ไพไรต์ที่ใช้ในการศึกษามาจากเหมืองทองคำ อำเภอทับคล้อ จังหวัดพิจิตร ซึ่งตั้งอยู่ทางตอนเหนือของประเทศไทย โดยก่อนที่จะนำตัวอย่างแร่มาทำการทดลองนั้น ต้องทำการเตรียมตัวอย่างโดยที่นำตัวอย่างแร่ไพไรต์มาบด และผ่านตะแกรงให้ได้ขนาดของแร่เป็น 425-850 ไมครอน หลังจากนั้นนำไปผสมกับทรายขนาด 1-2 มิลลิเมตร ในอัตราส่วน 1 : 4 สำหรับกระบวนการทดลองนั้น ประกอบด้วย การเคลือบผิว และการชะล้าง โดยที่การเคลือบผิวนั้นทดลองขึ้นเพื่อกำหนดสภาวะที่เหมาะสมต่อการสร้างเปลือกฟอสเฟตเคลือบผิวด้วยการใช้สารละลายที่ใช้ในการเคลือบผิว ซึ่งประกอบด้วยไฮโดรเจนเปอร์ออกไซด์ ( $H_2O_2$ ) โซเดียมอะซิเตด (NaAc) และโพแทสเซียมไฮโดรเจนฟอสเฟด ( $KH_2PO_4$ ) ที่มีความเข้มข้นต่างกัน และทดลองที่เวลาต่าง ๆ กัน ส่วนกระบวนการชะล้างนั้นทำการศึกษาในอ่างคอลัมน์เพื่อทดสอบความทนทานของตัวอย่างแร่ไพไรต์ที่เคลือบผิวแล้วต่อสภาวะออกซิไดซ์ ด้วยการใส่สารละลายที่มีคุณสมบัติเป็นตัวออกซิไดซ์ที่ดีซึ่งมีความเข้มข้นเป็น 0.145 M ชะล้างที่เวลาต่าง ๆ กัน หลังจากทำการทดลองการเคลือบผิว และการชะล้างแล้ว ตัวอย่างของสารละลายที่เก็บได้หลังจากการเคลือบผิวนั้น จะถูกนำไปวิเคราะห์หาค่าความเป็นกรด-ด่าง (pH) ปริมาณฟอสเฟต และปริมาณเหล็กที่หลุดออกมาจากผิวของแร่

จากการศึกษาทั้งหมด สรุปได้ว่าสภาวะที่เหมาะสมต่อการสร้างเปลือกฟอสเฟตเคลือบผิวของแร่ไพไรต์นั้นคือ การใช้สารละลายเคลือบผิวที่มีความเข้มข้นเป็น  $0.3 \text{ M } KH_2PO_4 + 0.2 \text{ M } H_2O_2 + 0.2 \text{ M } NaAc$  โดยมีค่าความเป็นกรด-ด่าง (pH) อยู่ในช่วง 5.46 ถึง 5.51 และมีปริมาณฟอสเฟตที่เหลืออยู่ในสารละลายน้อยที่สุด 0.497 - 0.745 มิลลิกรัมต่อลิตร หลังจากผ่านการชะล้าง มีค่าความเป็นกรด-ด่าง (pH) อยู่ในช่วง 6.45 ถึง 7.23 และมีแนวโน้มของปริมาณเหล็กลดลงซึ่งอยู่ในช่วง 0.008 - 0.151 มิลลิกรัมต่อลิตร นอกจากนี้ เมื่อวิเคราะห์ด้วยเครื่องมือ EPMA พบว่ามีปริมาณของฟอสเฟตที่เคลือบอยู่ที่ผิวของแร่ไพไรต์มากที่สุด สารละลายเคลือบผิวดังกล่าวถูกนำมาทดสอบกับดินเหลือทิ้งจากเหมืองถ่านหินซึ่งปรากฏผลที่น่าพอใจ แต่การศึกษารายละเอียดและปัจจัยทางเศรษฐกิจควรมานำมาพิจารณาต่อไป

สาขาวิชา การจัดการสิ่งแวดล้อม (สหสาขาวิชา)

ปีการศึกษา 2548

ลายมือชื่อนิพนธ์..... จันทรา กงมาก

ลายมือชื่ออาจารย์ที่ปรึกษา.....

ลายมือชื่ออาจารย์ที่ปรึกษาร่วม.....

# # 4689439320 : MAJOR ENVIRONMENTAL MANAGEMENT

KEY WORD: ACID MINE DRAINAGE / PYRITE OXIDATION / IRON-PHOSPHATE COATING

NIPON KONGMAK : ACID MINE DRAINAGE PREVENTION BY SUPPRESSION OF  
PYRITE OXIDATION WITH IRON-PHOSPHATE COATING ON PYRITE SURFACES.

THESIS ADVISOR : CHANTRA TONGCUMPOU, Ph.D., THESIS COADVISOR :  
ASST.PROF. CHAKKAPHAN SUTTHIRAT, Ph.D., 97 pp. ISBN 974-17-5756-5.

This study was aimed to examine the feasibility and determining the optimum condition of creating an iron-phosphate coating on pyrite surfaces for inhibiting pyrite oxidation and preventing acid mine drainage (AMD). Pyrite used in this study was collected from the gold mine, Amphoe Thap Khlo, Changwat Phichit (Akara Mining Limited), northern Thailand. Prior to the experiments, pyrite samples (425-850  $\mu\text{m}$ ) were mixed with sand in average size of 1-2 mm in ratios 1:4 for preparing samples. The experimental procedures comprise the coating process and leaching study. Coating process was conducted in batches by treating with various coating solution containing hydrogen peroxide ( $\text{H}_2\text{O}_2$ ), sodium acetate (NaAc) and potassium hydrogen phosphate ( $\text{KH}_2\text{PO}_4$ ) at different contact times for determining the optimum condition for coating at different conditions. Leaching study was performed in columns, 10 mm of diameter by leaching with 0.145 M of the oxidizing solution at different times for examining the resistance of coated pyrite to oxidizing condition. Phosphate remains, iron released and pH were analyzed for estimating the degree of pyrite oxidation.

The results of this study show that treating with the coating solution B (0.3 M  $\text{KH}_2\text{PO}_4$  + 0.2 M  $\text{H}_2\text{O}_2$  + 0.2 M NaAc) at the time of t20 is the optimum condition for establishing iron-phosphate formation on pyrite surfaces. Phosphate remains in solution is the lowest concentration after coating process (0.497 - 0.745 mg/l). pH ranges from 6.45 to 7.23 and iron released in leachate tends to be low concentration (0.008-0.151 mg/l). In addition, the quantity of phosphate coated on the pyrite surface analyzed using Electron Probe Micro Analyzer (EPMA) is the highest. Solution B was consequently applied to soil mining waste from coal mine which it yielded satisfactory result. However, detailed study and economic concern would be taken into account.

Field of study Environmental Management  
(Inter-Department)

Academic year 2005

Student's signature..... *Nipon Kongmak*

Advisor's signature..... *Ch. T.*

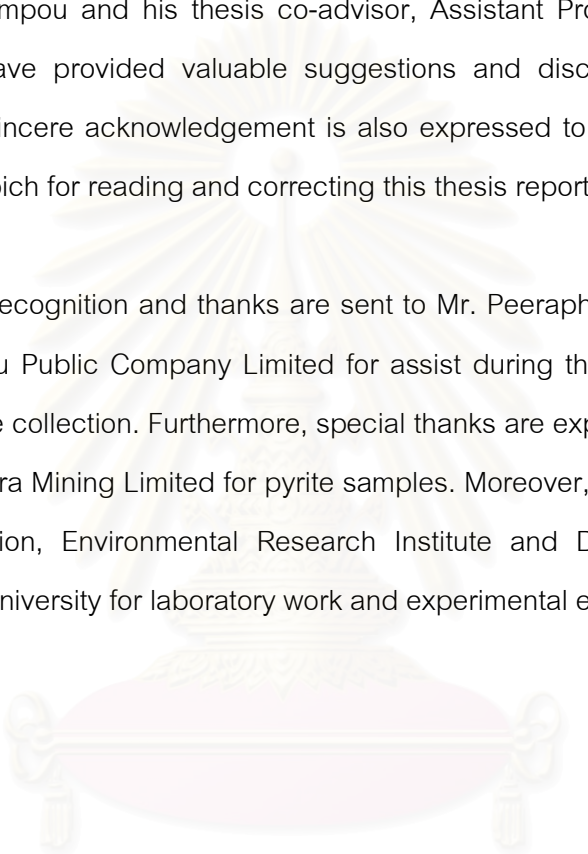
Co-advisor's signature..... *C. S. H.*

## ACKNOWLEDGEMENTS

The author's master study is financially supported by the National Research Center for Environmental and Hazardous Waste Management (NRC-EHWM).

The author would like to express his deeply grateful to his thesis advisor, Dr. Chantra Tongcumpou and his thesis co-advisor, Assistant Professor Dr. Chakkaphan Sutthirat who have provided valuable suggestions and discussions throughout this study. A great sincere acknowledgement is also expressed to Associate Professor Dr. Wasant Pongsapich for reading and correcting this thesis report.

Special recognition and thanks are sent to Mr. Peeraphol Nontakaew and other officers of Banpu Public Company Limited for assist during the field study, pyrite and soil mining waste collection. Furthermore, special thanks are expressed to Mr. Weerasak Lanwongsa, Akara Mining Limited for pyrite samples. Moreover, thanks are also given to Laboratory Section, Environmental Research Institute and Department of Geology, Chulalongkorn University for laboratory work and experimental equipments.



สถาบันวิทยบริการ  
จุฬาลงกรณ์มหาวิทยาลัย

# CONTENTS

	Page
ABSTRACT IN THAI.....	iv
ABSTRACT IN ENGLISH.....	v
ACKNOWLEDGEMENTS.....	vi
CONTENTS.....	vii
LIST OF TABLES.....	ix
LIST OF FIGURES.....	x
CHAPTER I INTRODUCTION.....	1
1.1 Statement of Problem.....	1
1.2 Objectives.....	4
1.3 Hypotheses.....	4
1.4 Scopes of the Study.....	4
1.5 Methodology.....	5
CHAPTER II THEORETICAL BAVKGROUND AND LITERATURE REVIEWS.....	8
2.1 Acid Mine Drainage (AMD) .....	8
2.1.1 Cause of AMD.....	8
2.1.2 Factors Affecting AMD Generation.....	10
2.1.3 Effects of Heavy Metal on the Environment.....	15
2.1.4 Hydrological Impact.....	15
2.1.5 General Prevention and Remediation Methods of AMD.....	16
2.2 Coating Technique with Iron - Phosphate.....	21
CHAPTER III METHODOLOGY.....	24
3.1 Materials.....	24
3.2 Experiment Procedures.....	24
3.2.1 Pyrite Sample Preparation.....	25
3.2.2 Coating Process.....	25

	Page
3.2.3 Leaching Study .....	28
3.3 Analysis Methods .....	31
3.3.1 Ascorbic Acid Method .....	32
3.3.2 Metals by Flame Atomic Absorption Spectrometry.....	35
3.3.3 Electron Probe Micro Analyzer (EPMA).....	36
3.4 Application with the Soil Mining Wastes.....	40
CHAPTER IV RESULTS AND DISCUSSION.....	43
4.1 Iron-phosphate Coating on Pyrite Surfaces Using Various Coating Solutions.....	43
4.1.1 Effect of potassium hydrogen phosphate ( $\text{KH}_2\text{PO}_4$ ) on creating an iron-phosphate coating.....	45
4.1.2 Effect of hydrogen peroxide ( $\text{H}_2\text{O}_2$ ) on creating an iron-phosphate coating.....	47
4.2 Chemical Composition on the Surfaces of Coated Pyrite.....	49
4.3 Resistance of the Coated Pyrite to Oxidizing Condition.....	54
4.4 Application for Soil Mining Wastes.....	67
CHAPTER V CONCLUSIONS AND SUGGESTIONS FOR THE FURTHER STUDIES.....	72
5.1 Conclusions.....	72
5.2 Suggestions for the Further Studies.....	73
REFERENCES.....	75
APPENDIX.....	77
BIOGRAPHY.....	98

## LIST OF TABLES

Table	Page
4.1 pH in solutions remained after treating with varying coating solutions at different contact times.....	44
4.2 Phosphate remaining in solutions after treating with various coating solutions at different contact times.....	46
4.3 The average of mass proportion on pyrite surfaces after analyzed using EPMA coating with solutions B, C, D and E .....	50
4.4 The average of atomic proportion on pyrite surfaces after coating with solutions B, C, D and E .....	50
4.5 pH in leachates of selected samples after leaching with 0.145 M of hydrogen peroxide solution (H <sub>2</sub> O <sub>2</sub> ) at different times.....	56
4.6 Iron released in leachates of selected samples after leaching with 0.145 M of hydrogen peroxide solution (H <sub>2</sub> O <sub>2</sub> ) at different times.....	56
4.7 Cumulative iron released in leachates of selected samples after leaching with 0.145 M of hydrogen peroxide solution (H <sub>2</sub> O <sub>2</sub> ) at different times.....	63
4.8 pH of leachates after treating with 200 ml of the coating solution (0.2 M KH <sub>2</sub> PO <sub>4</sub> + 0.2 M H <sub>2</sub> O <sub>2</sub> + 0.2 M NaAc) in columns 50 x 500 mm.....	67
4.9 pH of leachates after leaching with 100 ml oxidizing solution (0.2 M H <sub>2</sub> O <sub>2</sub> ) at different times (every 24 hours) in columns 50 x 500 mm.....	68
4.10 Iron released in leachates after leaching with 100 ml oxidizing solution (0.2 M H <sub>2</sub> O <sub>2</sub> ) at different times (every 24 hours) in columns 50 x 500 mm.....	69
4.11 Cumulative iron released from soil mining wastes after leaching with the oxidizing solution at different times.....	70

## LIST OF FIGURES

Figure	Page
1.1 Acid Mine Drainage (AMD) problem occurring at Amphoe Lee coal mine, Changwat Lumphun, northern Thailand (Banpu Public Company Limited).....	3
1.2 The simplified flow chart illustrating the methodology of the study .....	7
2.1 The examples of acid mine drainage (AMD) passive treatment provide alkalinity and reduce heavy metal loading; a) Open limestone channels, b) Aerobic wetland, c) Anoxic limestone drains and d) Diversion well (Seif, 1994) .....	20
3.1 Pyrite samples (425-850 $\mu\text{m}$ ) and sand (1 - 2 mm) before coating.....	25
3.2 The simplified flow chart exhibiting the coating process (Evangelou and Huang, 1992).....	28
3.3 Simplified flow chart illustrating the steps of leaching study .....	30
3.4 Leaching test in column with 10 mm of diameter x 400 mm long .....	31
3.5 Flow chart displaying the analysis procedures.....	33
3.6 Effects produced by electron bombardment of a material (Available from : <a href="http://www.cameca.fr">www.cameca.fr</a> ).....	37
3.7 Electromagnetic spectrum (Available from : <a href="http://www.cameca.fr">www.cameca.fr</a> ).....	38
3.8 Electron Probe Micro Analyzer (EPMA) used for analyzing the chemical composition on the pyrite surface (Available from : <a href="http://www.hardcoatings.ac.at">www.hardcoatings.ac.at</a> ).....	39
3.9 Simplified flow chart showing the steps of application with soil mining wastes.....	41
3.10 Application with the soil mining wastes studied in column with 50 mm of diameter x 500 mm long.....	42
4.1 Trends of pH value measured after treating with various coating solutions at different contact times (at the time of $t_0$ is the pH value after rinsing with distilled water before adding coating solution).....	45
4.2 Variation of remaining phosphate concentration after treating with various coating solutions at different contact times.....	47
4.3 Secondary electron image of non-coated pyrite illustrating the surface of pyrite (C = clay mineral, S = pyrite).....	51

Figure	Page
4.4 Secondary electron image of the pyrite coated by solution B illustrating iron-phosphate coating on the surface of pyrite (S = pyrite, P = iron-phosphate) ...	51
4.5 Secondary electron image of the coated pyrite using solution C illustrating iron-phosphate on the surface of pyrite (S = pyrite, P = iron-phosphate) .....	52
4.6 Secondary electron image of the coated pyrite using solution D illustrating iron-phosphate on the surface of pyrite (S = pyrite, P = iron-phosphate) .....	52
4.7 Secondary electron image of the coated pyrite using solution E illustrating iron-phosphate on the surface of pyrite (S = pyrite, P = iron-phosphate) .....	53
4.8 Trend of iron released in leachate of uncoted pyrite after leaching with 0.145 M of H <sub>2</sub> O <sub>2</sub> solution (H <sub>2</sub> O <sub>2</sub> ) at different times.....	57
4.9 Trends of pH and iron released in leachates of selected samples solution A after leaching with 0.145 M of H <sub>2</sub> O <sub>2</sub> solution (H <sub>2</sub> O <sub>2</sub> ) at different times.....	58
4.10 Trends of pH and iron released in leachates of selected samples solution B after leaching with 0.145 M of H <sub>2</sub> O <sub>2</sub> solution (H <sub>2</sub> O <sub>2</sub> ) at different times .....	59
4.11 Trends of pH and iron released in leachates of selected samples solution C after leaching with 0.145 M of H <sub>2</sub> O <sub>2</sub> solution (H <sub>2</sub> O <sub>2</sub> ) at different times.....	60
4.12 Trends of pH and iron released in leachates of selected samples solution D after leaching with 0.145 M of H <sub>2</sub> O <sub>2</sub> solution (H <sub>2</sub> O <sub>2</sub> ) at different times.....	61
4.13 Trends of pH and iron released in leachates of selected samples solution E after leaching with 0.145 M of H <sub>2</sub> O <sub>2</sub> solution (H <sub>2</sub> O <sub>2</sub> ) at different times.....	62
4.14 The trends of cumulative iron released of selected samples after leaching with 0.145 M of hydrogen peroxide solution (H <sub>2</sub> O <sub>2</sub> ) at different times.....	64
4.15 The trends of cumulative iron released of samples with the optimum time for coating process after leaching with 0.145 M of hydrogen peroxide solution (H <sub>2</sub> O <sub>2</sub> ) at different times.....	65
4.16 Trend of pH value after leaching with 100 ml oxidizing solution (0.2 M H <sub>2</sub> O <sub>2</sub> ) at different times (every 24 hours) in columns 50 x 500 mm.....	68
4.17 Iron concentrations after leaching with 100 ml oxidizing solution (0.2 M H <sub>2</sub> O <sub>2</sub> ) at different times (every 24 hours) in columns 50 x 500 mm.....	69

Figure

Page

4.18 Cumulative iron released from soil mining wastes after leaching with the oxidizing solution at different times.....	70
---	----



สถาบันวิทยบริการ  
จุฬาลงกรณ์มหาวิทยาลัย

# CHAPTER I

## INTRODUCTION

### 1.1 Statement of Problem

At mining sites, the major pollutant sources of concern are waste rock or overburden disposals, tailings, dump leaches and mine water. Waste rock or overburden is the soil and rock mining operations move during the process of accessing a mineral body. It also includes rock removed while sinking shafts and exploiting the mineral body and rock bedded with mineral. The size of waste rock ranges from small clay particles to boulders. Most of the waste rock generated is disposed of in piles near the mine site (Garcin, 2003).

Tailings are the waste solids remaining after beneficiation of ore through a variety of milling processes. After ore is extracted from a mine, the first step in a beneficial mining process is generally crushing and grinding. The crushed ores are then concentrated to free the valuable mineral and metal particles from the less valuable rock. Beneficiation processes include physical or chemical separation techniques such as gravity concentration, magnetic separation, electrostatic separation, flotation, solvent extraction, precipitation and amalgamation. In most cases, mine tailings are disposed in onsite impoundments such as tailing ponds (Garcin, 2003).

Leaching is another beneficial process commonly used to recover certain metals such as gold, silver, copper and uranium from their minerals. The type of leaching solution used depends on the characteristics of the mineral. As the liquid percolates through the mineral, it leaches out metals. Dump leach piles can be very large. Heap leaching is used for higher valuable ores and is generally smaller than dump leach operations. Almost regularly, there are one or more impermeable liners under the leach material to maximize recovery of the leachates. When leaching no longer produces economically attractive quantities of valuable metals, the spent mineral is left in place after rinsing or other detoxification process (Garcin, 2003).

Acid generation and metals dissolution are the primary problems associated with pollution from mining activities. The chemistry of these processes appears simple, but quickly becomes complicated as geochemist and physical characteristics can vary greatly from site to site (Garcin, 2003).

Acid Mine Drainage (AMD) is a natural occurrence resulting from the exposure of sulfur and iron bearing materials to erosion and weather. Percolation of water through these materials results in a discharge with low pH and high metals concentration. Although AMD is a naturally occurring process, mining activities may greatly accelerate its production. AMD production is accelerated since mining exposes new iron and sulfide surfaces; for example, underground mine walls, open pit walls and overburden and mine waste piles to oxygen. Therefore, AMD is one of the primary environmental threats at mining sites (Garcin, 2003).

At Amphoe Lee coal mine, Changwat Lumphun, northern Thailand (Banpu Public Company Limited), Acid Mine Drainage (AMD) is the most significant environmental problem after closure of the mine site. Open limestone channels and the application of limestone are used for neutralizing acidity and precipitating iron in order to prevent acid generation and metals dissolution at mining sites. In addition, diversion wells, anoxic limestone drains, aerobic wetlands and use of bactericides, phosphate and various liners; for example, plastic and clay liners for the purpose of inhibiting  $\text{Fe}^{3+}$  or  $\text{O}_2$  from coming into contact with metal - sulfides are alternative prevention methods of AMD. However, these approaches for preventing AMD have short-term of effectiveness because of the fact that the surfaces of metal - sulfides remain exposed to the oxygen after treatment. In this research, coating with iron-phosphate is a new technique for the abatement of AMD (Georgopoulou et al., 1995). The coating process is based on the hypothesis that when a pyrite is treated with a phosphate solution containing hydrogen peroxide,  $\text{H}_2\text{O}_2$ , it results in oxidation and ferric iron released ( $\text{Fe}^{3+}$ ) will react with the phosphate ions. A passive coating on the pyrite surface is thus formed. Therefore, pyrite oxidation and acid production will stop. It appears to be a long-term solution for the preventing of AMD (Georgopoulou et al., 1995).



Figure 1.1 Acid Mine Drainage (AMD) problem occurring at Amphoe Lee Coal mine, Changwat Lumphun, northern Thailand (Banpu Public Company Limited).

จุฬาลงกรณ์มหาวิทยาลัย

## 1.2 Objectives

The objectives of this research can be divided into two points as follows:

1.2.1 The main objective was to examine the feasibility of creating an iron-phosphate coating on pyrite that inhibits pyrite oxidation.

1.2.2 The specific objectives were to determine the optimum conditions of creating iron-phosphate in the coating process and to examine the resistance of the coated pyrite to oxidizing conditions.

## 1.3 Hypotheses

Creating an iron-phosphate coating on a pyrite surface under the optimum condition can effectively inhibit pyrite oxidation.

## 1.4 Scopes of the Study

The research was conducted to examine the feasibility of creating an iron-phosphate coating on pyrite that will inhibit pyrite oxidation. The suitability of the application and its potential environmental impact is also addressed. The following points of the research were studied.

1.4.1 Pyrite used in the study came from a coal mine in Amphoe Lee, Changwat Lumphun (Banpu Public Company Limited) and a gold mine in Amphoe Thap Khlo, Changwat Phichit (Akara Mining Limited), northern Thailand.

1.4.2 Laboratory experiments were carried out through the coating process and leaching study in order to create iron-phosphate coating on pyrite surfaces and determine the resistance of the coated pyrite to an oxidizing environment. These experiments were divided into two parts as follows:

1.4.2.1 The coating process was investigated for optimum conditions using various concentrations of coating solution at different contact periods.

1.4.2.2 A leaching study investigated leaching with the oxidizing solution at different contact periods.

1.4.3 Application of the optimum condition of creating an iron-phosphate coating on pyrite surfaces for soil mining wastes was carried out in order to estimate the effectiveness for preventing pyrite oxidation.

## 1.5 Methodology

The following procedures have been conducted in order to achieve the objectives of the study. The Figure 1.2 illustrates the flow chart of overall procedures for this study.

### 1.5.1 Literature reviews

Previous works related to this study were investigated for fundamental knowledge of Acid Mine Drainage (AMD) including processes, factors affecting AMD, effects of heavy metals on the environment, general remediation methods of AMD as well as coating technology for preventing AMD. Related research have been reviewed and analyzed to draw the scope of this study as well as to compare this work with previous studies.

### 1.5.2 Pyrite and soil sampling

According to the scopes of the study, pyrite was obtained from Amphoe Lee coal mine, Changwat Lumphun (Banpu Public Company Limited) and Amphoe Thap Khlo gold mine, Changwat Phichit (Akara Mining Limited), northern Thailand. Soils were gathered from mining waste or overburden layers at coal pits from Banpu Public Company Limited.

### 1.5.3 Laboratory study

This procedure was carried out through the coating process and leaching study in order to create an iron-phosphate coating on pyrite surfaces and to determine the resistance of the coated pyrite to an oxidizing environment. Moreover, the optimum condition of creating an iron-phosphate coating on pyrite surfaces was applied for soil mining wastes in order to estimate the effectiveness for preventing pyrite oxidation.

### 1.5.4 Analysis and discussion

The results of the laboratory experiments were analyzed and discussed in order to determine the optimum condition in creating an iron-phosphate coating on pyrite surfaces and estimating the effectiveness of the application for soil mining waste inhibiting Acid Mine Drainage (AMD).

### 1.5.5 Conclusions

After the laboratory study, analysis and discussion procedures have been done, whole data conclusions will be drawn. Suggestions raised in this research will be considered for further studies.

### 1.5.6 Thesis writing

Overall works done for this study were reported as a thesis book including chapters as follows; Chapter 1 introduction, Chapter 2 theoretical background and literature reviews, Chapter 3 methodology, Chapter 4 results and discussion, and Chapter 5 conclusions and suggestions for the further studies.

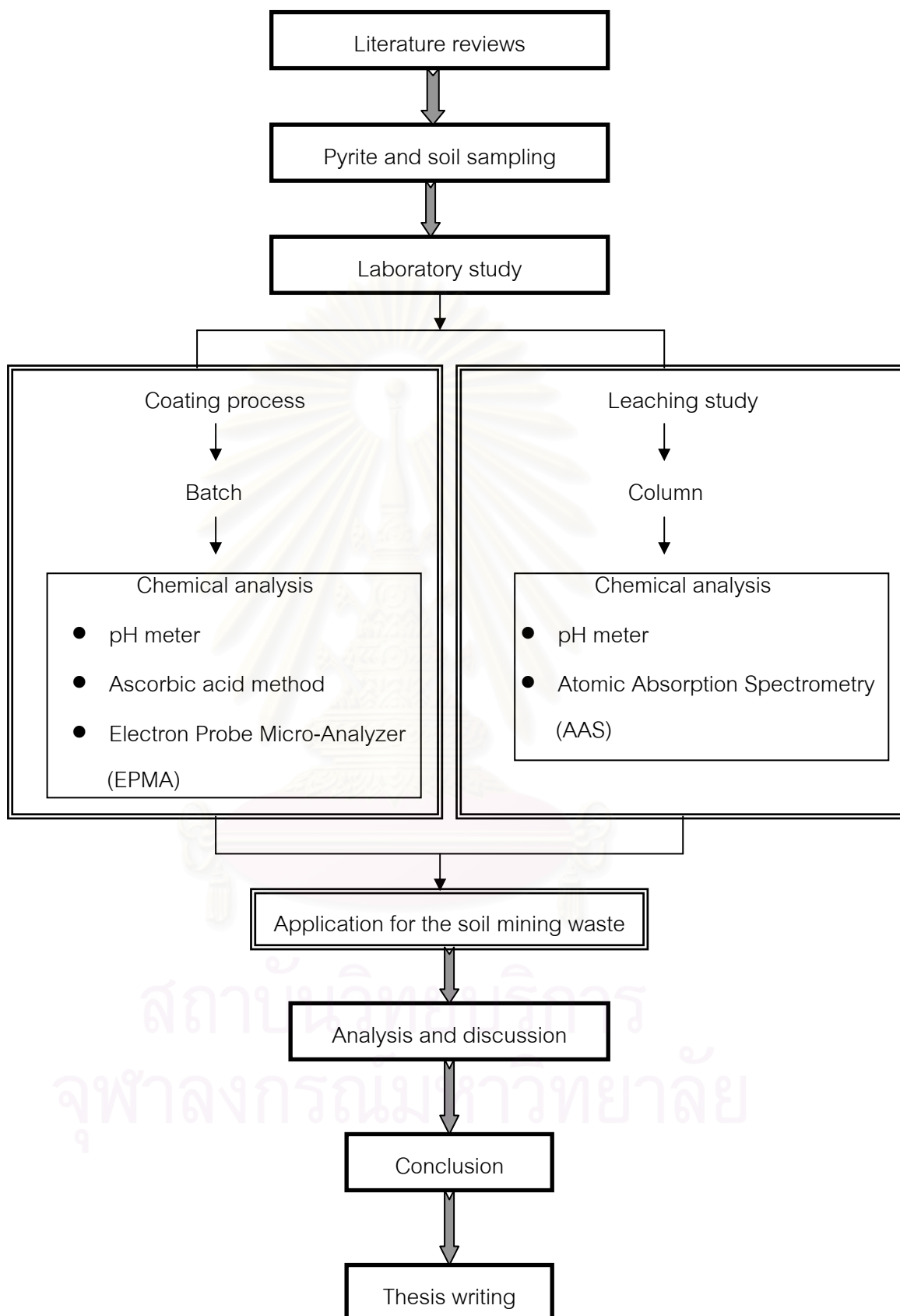


Figure 1.2 The simplified flow chart illustrating the methodology of the study.

## CHAPTER II

### THEORETICAL BACKGROUND AND LITERATURE REVIEWS

#### 2.1 Acid Mine Drainage (AMD)

Acid mine drainage (AMD) is one of the most significant environmental problems arising from both operating and closed mine sites. AMD is drainage flowing from or caused by surface mining, deep mining or coal refuse piles that is typically highly acidic with elevated levels of dissolved metals.

AMD, in which mineral acidity exceeds alkalinity, typically contains elevated concentrations of sulfate, Fe, Mn, Al and other ions. AMD may not necessarily have a low pH (high concentration of  $H^+$  ions), since the presence of dissolved Fe, Al and Mn can generate hydrogen ions by hydrolysis. The major source of acidity is oxidation of pyrite ( $FeS_2$ ) in freshly broken rock that is exposed by mining. Pyrite oxidation can be rapid upon exposure to humid air or aerated water, particularly above the water table. In contrast, neutral or alkaline mine drainage has alkalinity that equals or exceeds acidity but can still have elevated concentrations of sulfate, Fe, Mn and other solutes. Neutral or alkaline mine drainage can originate as AMD that has been neutralized by reaction with carbonate minerals, such as calcite and dolomite, or can form from rock that contains little pyrite. Dissolution of carbonate minerals produces alkalinity, which promotes the removal of Fe, Al and other metal ions from solution, and neutralizes acidity. However, neutralization of AMD does not usually affect concentrations of sulfate (Seif, 1994).

##### 2.1.1 Cause of AMD

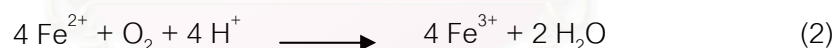
The formation of Acid Mine Drainage (AMD) is primarily a function of the geology, hydrology and mining technology employed at the mine site. AMD is formed by a series of complex geo-chemical and microbial reactions that occur when metal-sulfides in coal, refuse or the overburden of a mine operation are exposed to an

oxidizing environment, such as air and water. Pyrite ( $\text{FeS}_2$ ) is typically the most abundant metal-sulfide in coal mine waste and often exists in association with other heavy metals such as arsenic, cadmium, copper, zinc and lead (Monterroso and Macias, 1998). The resulting water is usually high in acidity and dissolved metals. The metals stay dissolved in solution until the pH rises to a level where precipitation occurs. Solubility charts for the various metals show the pH at which precipitation begins and the pH at which maximum insolubility occurs.

Pyrite oxidation is the major cause of acid mine drainage (AMD) that impairs surface and groundwater quality. Ferric iron,  $\text{Fe}^{3+}$ , and atmospheric oxygen,  $\text{O}_2$ , are the major pyrite oxidants. The reactions of pyrite oxidation are shown as follows: (Singer and Stumm, 1970)



The first reaction is the weathering of pyrite. Sulfur is oxidized to sulfate, while ferrous iron and acid are released. This reaction generates two moles of acid for each mole of pyrite oxidized.



The second reaction involves the conversion of ferrous iron to ferric iron consuming one mole of acidity. Certain bacteria increase the rate of oxidation from ferrous iron to ferric iron. The reaction rate is pH dependent, with the reaction proceeding slowly under acidic conditions (pH 2-3) without bacteria present but several orders of magnitude faster at pH values near 5. Thus, it is referred to as the "rate determining step" in the overall acid-generating sequence.



The third reaction is the hydrolysis of iron which splits the water molecule. Acidity is generated as a by product and many metals are capable of undergoing hydrolysis. The formation of ferric hydroxide precipitate, commonly referred to as yellow boy, is pH dependent. Solids form when the pH is above 3.5 while solids will not precipitate below pH 3.5.



The fourth reaction is the oxidation of additional pyrite by ferric iron which is generated in reactions (1) and (2). This is the cyclic and self propagating part of the overall reaction and takes place very rapidly and continues until either ferric iron or pyrite is depleted. In this reaction iron is the oxidizing agent, not oxygen.



An overall summary reaction of pyrite oxidation is shown in the fifth equation.

### 2.1.2 Factors Affecting AMD Generation

The potential for a mine or its associated waste to generate acid and release contaminants depends on many factors and is site-specific. These site-specific factors can be categorized as generation factors, control factors and physical factors (Garcin, 2003).

#### 2.1.2.1 Generation factors

Generation factors determine the ability of the material to produce acid. Water and oxygen are necessary to generate AMD. Certain bacteria enhance acid generation. Water serves as a reactant, a medium for bacteria and the transport medium for the oxidation products. A ready supply of atmospheric oxygen is required to drive the oxidation reaction. Oxygen is particularly important in maintaining the rapid oxidation

catalyzed by bacteria at pH values below 3.5. Oxidation of sulfides is significantly reduced when the concentration of oxygen in the pore spaces of mining waste units is less than 1 or 2 percent. Different bacteria are better suited to different pH levels and physical factors. The type of bacteria and population sizes change as growth conditions are optimized.

**Effect of oxygen** – Atmospheric oxygen is required for the direct oxidation of pyrite and for regeneration of  $\text{Fe}^{3+}$ . Thus, if air and oxygenated or  $\text{Fe}^{3+}$ , rich waters can be excluded from pyritic material, pyrite oxidation can be inhibited and little or no acid will be generated. Pure water in equilibrium with air at a total pressure of 1 atmosphere contains relatively low concentrations of dissolved  $\text{O}_2$  ranging from 7.5 mg/L at 30 °C to 12.4 mg/L at 5 °C. Higher concentrations of the products require additional  $\text{O}_2$  transfer from the air or a more complex mechanism such as oxidation by previously generated  $\text{Fe}^{3+}$ .

Because the diffusion of  $\text{O}_2$  in water is a slow process and the solubility of  $\text{O}_2$  in water is low, the effective exclusion of atmospheric  $\text{O}_2$  from pyritic spoil can be achieved by perpetual immersion of the spoil in stagnant ground water. Conversely, most AMD is generated in unsaturated mine spoil or other environments where air is in contact with moist pyrite-bearing rock. Exclusion of  $\text{O}_2$  by construction of "impermeable" or organic-rich covers has not generally been successful in preventing AMD generation in unsaturated spoil or mine workings. Covers may fail to stop or slow AMD formation because  $\text{O}_2$  transfer is difficult to eliminate and because the rate of pyrite oxidation is independent of  $\text{O}_2$  concentrations over the range of 21 to 0.5 volume percent. In the unsaturated zone,  $\text{O}_2$  can be supplied relatively rapidly by advection of air resulting from barometric pumping or differences in temperature and by molecular diffusion through air-filled pores.

**Bacteria** - In many situations, the most important control on rate of AMD generation is bacterial oxidation of  $\text{Fe}^{2+}$  to  $\text{Fe}^{3+}$  by reaction (2) in the pyrite oxidation reaction. The resultant  $\text{Fe}^{3+}$  can oxidize pyrite by reaction (4).

The bacterium *Thiobacillus ferrooxidans* and several similar species have the capability of catalyzing  $\text{Fe}^{2+}$  oxidation (reaction 2) under acidic or aerobic conditions, and obtain the energy for their metabolism from this reaction. In the process, these bacteria greatly speed up the reaction, so that under optimum conditions the "half-life" of  $\text{Fe}^{2+}$  is decreased to about two hours in an aerated solution with pH of about 2.0 and Fe concentration of about 2.5 g/l. Because the rate of pyrite oxidation by  $\text{Fe}^{3+}$  is generally fast relative to the rate of oxidation by  $\text{O}_2$  or the rate of inorganic  $\text{Fe}^{2+}$  to  $\text{Fe}^{3+}$  oxidation, the  $\text{Fe}^{2+}$  -  $\text{Fe}^{3+}$  oxidation is commonly rate-controlling (Singer and Stumm, 1970), and the bacteria are crucial in determining the rate of acid formation. In addition to oxidation of dissolved  $\text{Fe}^{2+}$ , Thiobacilli also have the ability to oxidize pyrite directly, i.e., they can accomplish reaction (1) in the pyrite oxidation reaction while directly attached to the pyrite surface.

**Effect of temperature** - In general, the rates of reactions that form AMD increase with increasing temperature, so that AMD is formed faster if the pyritic material is warm. An exception to this trend is the rate of Fe oxidation by *T. ferrooxidans* above about 35°C. These bacteria thrive at optimum temperatures of 25 to 35 °C, but they become inactive or die as temperatures increase to about 55°C. Measurements indicate that oxidizing sulfide-rich material can warm internally to temperatures at least as high as 60°C because of the heat released by the oxidation reactions. Some sulfide-rich material actually undergoes spontaneous combustion.

**Effect of pH** - As indicated above, at pH values of 4 to 7 the rate of pyrite oxidation by  $\text{O}_2$  is slow, and  $\text{Fe}^{3+}$  concentration is limited by the low solubility of  $\text{Fe}(\text{OH})_3$ . Since  $\text{Fe}^{3+}$  can rapidly oxidize pyrite, the oxidation of pyrite can be greatly accelerated at low pH. However, below about pH 1.5 to 2 the effectiveness of *Thiobacillus ferrooxidans* as a catalyst of  $\text{Fe}^{2+}$  oxidation decreases. Although pH values as low as negative 1.4 have been observed for AMD, these low values seem to require special circumstances.

Kleinmann et al. (1981) have suggested that the generation of AMD can be understood as three sequential stages. In stage I, while the pH is near-neutral or only slightly acidic, pyrite oxidation by reaction (1) in the pyrite oxidation reaction proceeds by a combination of abiotic and bacterial mechanisms, and  $\text{Fe}^{2+}$  oxidation is primarily abiotic. Any biotic oxidation of pyrite is dominantly by bacteria attached to the surface of pyrite grains. In stage II, pH is generally in the range of 3 to 4.5, and  $\text{Fe}^{2+}$  oxidation is mainly by *T. ferrooxidans*, because abiotic oxidation is so slow. Pyrite oxidation in this transition stage occurs by a combination of reactions (1) and (4), both abiotically and bacterially. In stage III, at pH of less than about 3, the concentration of  $\text{Fe}^{3+}$  becomes high enough that reaction (4) becomes the main mechanism for acid production, with bacterial reoxidation of  $\text{Fe}^{2+}$  furnishing the  $\text{Fe}^{3+}$ . In stages I and II, the rate of AMD generation is relatively slow, but in stage III the rate becomes very rapid. This stage is responsible for production of the most acidic AMD. It should be noted that this sequence is based on processes in unsaturated systems with an adequate supply of  $\text{O}_2$  and negligible alkaline material. In environments of limited  $\text{O}_2$  and significant carbonate or other alkaline material, a different sequence of processes may occur.

#### 2.1.2.2 Chemical control factors

These factors determine the products of the oxidation reaction. They include the ability of the generation rock or receiving water to either neutralize the acid or to change the effluent character by adding metals ions mobilized by residual acid. Neutralization of acid by the alkalinity released when acid reacts with carbonate minerals is an important means of moderating acid production and can serve to delay the onset of acid production for long periods or even indefinitely. The most common neutralizing minerals are calcite and dolomite. Products from the oxidation reaction, such as hydrogen ions and metal ions, may also react with other non-neutralizing constituents. Possible reactions include ion exchange on clay particles, gypsum precipitation and dissolution of other minerals. The dissolution of other minerals contributes to the contaminant load in the acid drainage. Examples of metals occurring in dissolved form include aluminum, manganese, copper, lead, zinc and others.

**Effect of microenvironments** - Within unsaturated spoil, water typically fills small pores and occurs as film on particle surfaces. Flow rates of the water vary from relatively rapid movement through interconnected large pores, fractures, and joints to slow movement or nearly stagnant conditions in water films or small pores. Also, the abundance and distribution of pyrite and other minerals varies from one particle to another. Volumes with abundant pyrite, free movement of air, and impeded movement of water are expected to develop higher acidities than equal volumes that contain less pyrite or that are completely saturated with water. In addition, *T. ferrooxidans* may attach directly to pyrite surfaces and create its own microenvironment favorable to oxidation.

Because of these factors, the chemical environment within spoil, and consequently, water quality in unsaturated and saturated spoil commonly exhibit spatial and temporal variability. Because of the small dimensions of the varying chemical environments, thorough characterization of chemical conditions (pH, O<sub>2</sub> and Fe<sup>3+</sup>) in unsaturated spoil may not be possible.

#### 2.1.2.3 Physical factors

The second factors include the physical characteristics of the waste or structure, the way in which acid generating and acid neutralizing materials are placed and the local hydrology as well as geohydrology. The physical nature of the material such as particle size, permeability and physical weathering characteristics is important to the acid generation potential. Although difficult to measure, each of these factors influence the potential for acid generation is an important consideration for long term waste management. Particle size is a fundamental concern because it affects the surface area exposed to weathering and oxidation. Surface area is inversely proportional to particle size. The relationships among particle size, surface area and oxidation play a prominent role in acid production methods and in mining waste management units. As waste material weathers with time, particle size is reduced, exposing a greater surface area and changing the physical characteristics of the waste unit. However, this is a slow process.

**Effect of pyrite surface area and crystallinity** - Kinetic studies indicate that the rate of acid generation depends on the surface area of pyrite exposed to solution, and on the crystallinity and chemical properties of the pyrite surface. This dependence will be most important in initial stages while pH is greater than about 2.5. In general, rock with a high percentage of pyrite will produce acidity faster than rock with a low percentage of pyrite. Also, a given mass of pyrite in small particles with high surface area will tend to oxidize more rapidly than the same mass composed of coarse, smooth-surfaced grains. The high surface area of framboidal pyrite at least partly accounts for its observed high reactivity.

### 2.1.3 Effects of Heavy Metal on the Environment

The term heavy metal refers to any metallic chemical element that has a relatively high density and is toxic or poisonous at low concentrations. Examples of heavy metals include mercury (Hg), cadmium (Cd), arsenic (As), chromium (Cr) and lead (Pb). When metals are in a dissolved form they are more easily absorbed and to be accumulated by plant and animal life, therefore generally more toxic than when they are in solid form. Sub-lethal negative effects can occur as these metals concentrations settle into streams, stream beds and banks. Because the transfer or uptake of metals can occur within animal tissues and plants, they can be passed along to other organism in the food chain.

Heavy metals can enter a water supply by Acid Mine Drainage (AMD) or even from acidic rain breaking down soils and releasing heavy metals into streams, lakes, rivers and groundwater. One potential source of dissolved pollutants is chemical usage in mining and beneficiation. Common types of reagents include copper, zinc, chromium, sulfuric acid at copper leaching operations (Garcin, 2003).

### 2.1.4 Hydrological Impact

The surface and subsurface hydrology of the area surrounding mine operations and waste units is important in the analysis of acid generation potential. Wetting and

drying cycles in any of the mine operations or other waste units will affect the character of any produced acid mine drainage. Frequent wetting will generate a more constant volume of acid and other contaminants as water moves through and flushes oxidation products out of the system. The build up of contaminants in the system is proportional to the length of time between wetting cycles. As the length of dry cycles increase, oxidation products will accumulate in the system. A high magnitude wetting event will then flush the accumulated contaminants out of the system. This relationship is typical of the increase in the contaminant load observed following heavy rainfall for those areas having a wet season. However, in underground mines, the acid generating material occurs below the water table and the slow diffusion of oxygen in water can retard acid production. During acid generation, the pH values of the associated waters typically decrease to pH values near 2.5. These conditions result in the dissolution of the minerals associated with the metallic sulfides and release of toxic metal cations, for example, lead, copper, silver, manganese, cadmium, iron and zinc. In addition, the concentration of dissolved anions such as sulfate also increases.

Acid generation and drainage affect both surface water and groundwater. The sources of surface water contamination are leachate from mine openings, seepage and discharges from waste rock, tailings or spent ore, groundwater seepage and surface water run-off from waste rock and tailings piles. It should also be noted that mined materials, waste rock or tailings, used for construction or other purposes such as road beds, rock drains and fill material or off a mine site can also develop acid mine drainage. The receptors of contaminated surface water include aquatic birds, fish and other aquatic organisms and humans. Direct ingestion of contaminated surface water or direct contact through outdoor activities such as swimming can affect humans. Fish, birds and other aquatic organism are potentially affected by bottom foraging and direct exposure to surface water (Garcin, 2003).

#### **2.1.5 General Prevention and Remediation Methods of AMD**

General prevention and remediation methods of acid mine drainage (AMD) are categorized into two ways as below (Seif, 1994):

#### 2.1.5.1 Active treatment

This treatment involves adding a neutralizing agent such as  $\text{CaCO}_3$ , NaOH or Sodium-bicarbonate directly to streams that have been impacted. In these treatment systems, the acidity is buffered by the addition of alkaline chemicals such as calcium carbonate, sodium hydroxide, sodium bicarbonate or anhydrous ammonia. These chemicals raise the pH to acceptable levels and decrease the solubility of dissolved metals. Precipitates form and settle from the solution.

However, these chemicals are expensive and the treatment system requires additional costs associated with operation and maintenance as well as the disposal of metal-laden sludges.

#### 2.1.5.2 Passive treatment

The approach includes a variety of techniques to raise the stream pH values and reduce heavy metals loading. For example, open limestone channels, diversion wells, anoxic limestone drains and aerobic wetlands. Passive treatment conceptually offers many advantages over conventional active treatment systems. The use of chemical addition and energy consuming treatment processes are virtually eliminated with passive treatment systems. Also, the operation and maintenance requirements of passive systems are considerably less than active treatment systems.

The first passive technology involved the use of natural *Sphagnum* wetlands that could improve the water quality of AMD without causing other detrimental impacts on the ecosystem. Although this concept had its limitations, it spawned research and development into other passive treatment technologies that did not follow the natural wetland paradigm.

Designing a passive treatment system for AMD requires the understanding of mine water chemistry, available treatment techniques and experience. Analytical sampling of the AMD is extremely important in the selection of appropriate treatment technologies.

### Open limestone channels

This method may be the simplest passive treatment. Open limestone channels are constructed in two ways. In the first method, a drainage ditch is constructed of limestone and AMD-contaminated water is collected by the ditch. The other method consists of placing limestone fragments directly in a contaminated stream. Dissolution of the limestone adds alkalinity to the water and raises the pH. Armoring or coating of the limestone by  $\text{Fe}(\text{CO})_3$  and  $\text{Fe}(\text{OH})_3$  produced by neutralization reduces the generation of alkalinity, so large quantities of limestone are needed to ensure long-term success. High flow velocity and turbulence enhance the performance by keeping precipitates in suspension thereby reducing the armoring of the limestone. Open limestone channels are sized according to standard engineering practice using the Manning equation and providing additional freeboard. Impervious liners are sometimes used under the limestone to prevent infiltration of the AMD into the groundwater table.

### Aerobic wetland

An aerobic wetland consists of a large surface area pond with horizontal surface flow. The pond may be planted with cattails and other wetland species. Aerobic wetlands can only effectively treat water that is net alkaline. In aerobic wetland systems, metals are precipitated through oxidation reactions to form oxides and hydroxides. This process is more efficient when the influent pH is greater than 5.5. Aeration increases the efficiency of the oxidation process and therefore the precipitation process. Iron concentrations are efficiently reduced in this system but the pH is further lowered by the oxidation reactions.

A typical aerobic wetland will have a water depth of 6 to 18 inches. Variations in water depth within the wetland cell may be beneficial for performance and longevity. Although shallow water zones freeze more quickly in winter, they enhance oxygenation, oxidizing reactions and precipitation. Deeper water zones provide storage areas for precipitates but decrease vegetative diversity.

### Anoxic limestone drains (ALD)

An anoxic limestone drain (ALD) is a buried bed of limestone constructed to intercept subsurface mine water flows and prevent contact with atmospheric oxygen. Keeping oxygen out of the water prevents oxidation of metals and armoring of the limestone. The process of limestone dissolution generates alkalinity. The purpose of an ALD is to provide alkalinity thereby changing net acid water into net alkaline water. Retaining carbon dioxide in the drain can improve limestone dissolution and alkalinity generation.

Anoxic limestone drains can be considered a pretreatment step to increase alkalinity and raise pH before the water enters a constructed aerobic wetland. In the aerobic wetland, metals can be oxidized and precipitated. ALD is limited by the amount of alkalinity they can generate based on solubility equilibrium reactions. Also, the effectiveness and longevity of an ALD can be substantially reduced if the acid mine drainage (AMD) has high concentrations of ferric iron, dissolved oxygen or aluminum.

### Diversion wells

This approach is another simple way of adding alkalinity to contaminated waters. Acidic water is conveyed by a pipe to a downstream "well" which contains crushed limestone aggregate. The hydraulic force of the pipe flow causes the limestone to turbulently mix and abrade into fine particles and prevent armoring. The water flows upward and overflows the "well" where it is diverted back into the stream. Diversion wells require frequent refilling with clean limestone to assure continued treatment.

Nevertheless, most of these methods for preventing AMD have short-term effectiveness because of the fact that surfaces of pyrite remain exposed to the atmosphere, to  $O_2$ , after treatment. These approaches include limestone application for neutralizing acidity and precipitating iron, use of bactericides, phosphate and various liners; for example, plastic and clay liners for the purpose of inhibiting  $Fe^{3+}$  or  $O_2$  from coming into contact with pyrite.

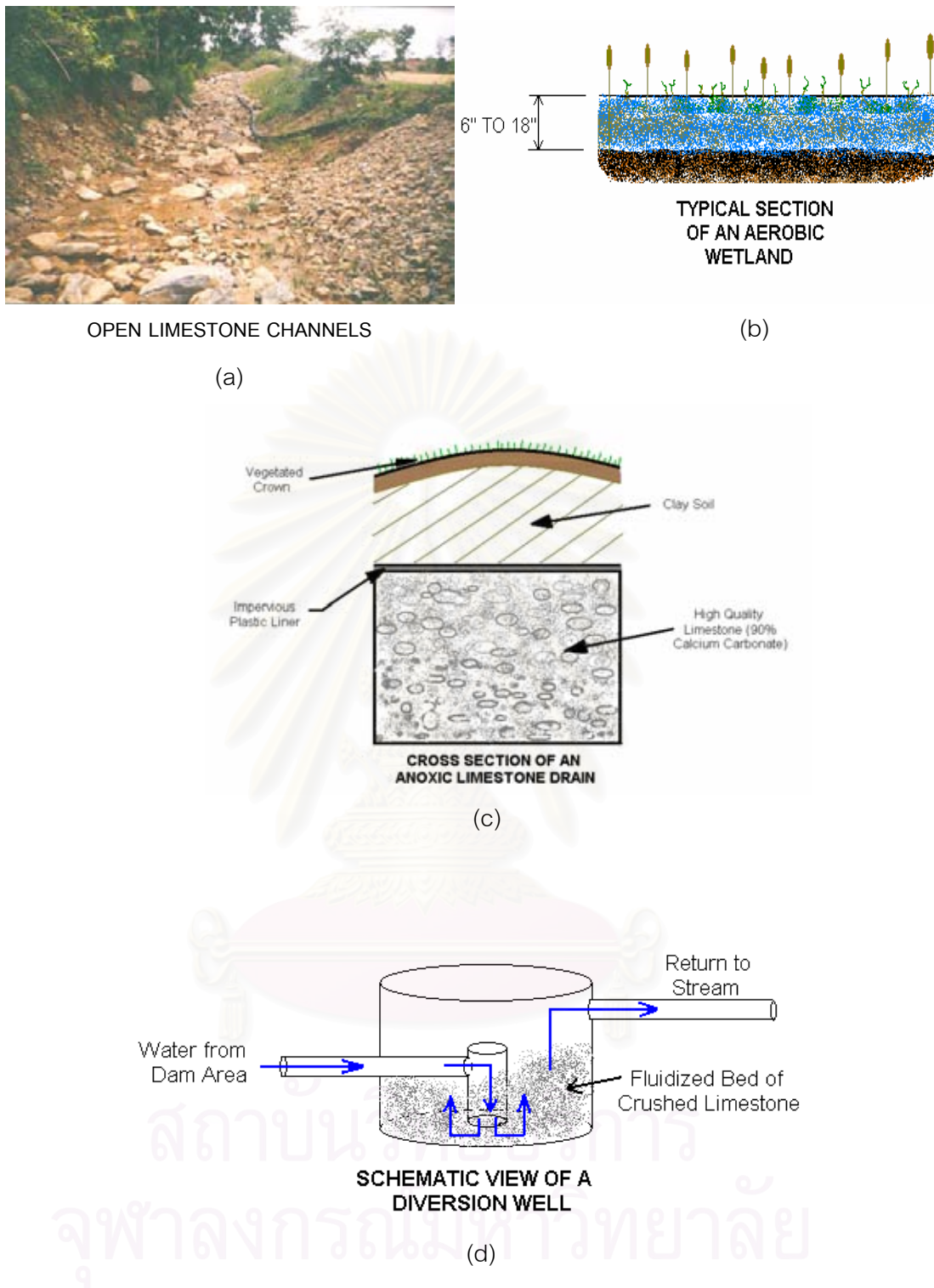


Figure 2.1 The examples of acid mine drainage (AMD) passive treatment provide alkalinity and reduce heavy metal loading; a) Open limestone channels b) Aerobic wetland, c) Anoxic limestone drains and d) Diversion wells (Seif, 1994).

## 2.2 Coating Technique with Iron - Phosphate

Coating with iron-phosphate is a new technique for the abatement of acid mine drainage (AMD). The pyrite coating process is based on the hypothesis that when pyrite is treated with a phosphate solution containing  $\text{H}_2\text{O}_2$ , oxidation will take place and ferric ions,  $\text{Fe}^{3+}$ , released will react with the phosphate ions. Passive coating on the pyrite surface is the result, therefore, pyrite oxidation and acid production will stop (Evangelou and Huang, 1992). It appears to be a long-term solution for the prevention of AMD. The method was first applied on framboidal or pulverized mineral pyrite particles.

When hydrogen peroxide,  $\text{H}_2\text{O}_2$ , is the oxidizing agent, the oxidation reaction is demonstrated as below (Singer and Stumm, 1970).



The process is an autocatalytic process as  $\text{Fe}^{3+}$  which is one of the oxidation products can also oxidize pyrite.

When phosphate solution in the form of  $\text{H}_2\text{PO}_4$  is presented along with  $\text{H}_2\text{O}_2$ , the oxidation reaction as an unbalanced equation can be written as:



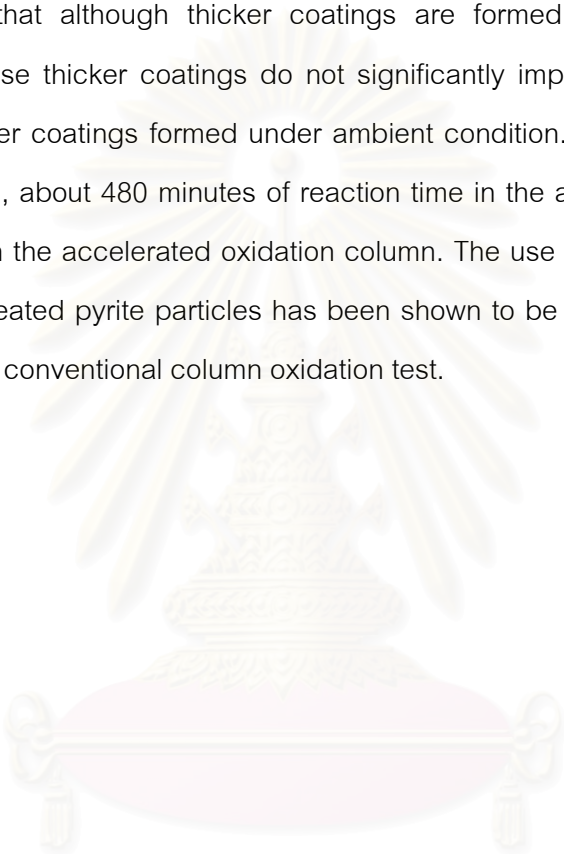
According to the reaction, iron phosphate will precipitate as a coating on the pyrite surface, depending of the degree of supersaturation.

Zhang and Evangelou (1998) investigated formation of ferric hydroxide-silica coatings on pyrite and its oxidation behavior in order to examine the feasibility of controlling pyrite oxidation in bench-scale studies by creating a ferric hydroxide-silica coating that would prevent either  $\text{O}_2$  or  $\text{Fe}^{3+}$  from oxidizing pyrite further. They concluded that ferric hydroxide-silica coating formation involved leaching pyrite at room temperature using a 10 mm chromatographic column with a solution containing  $\text{H}_2\text{O}_2$ ,

Na-acetate (NaOAC) and soluble silicate at a flow rate of  $0.43 \text{ ml min}^{-1}$ . The results of this bench-scale study show that formation of a ferric hydroxide-silica coating was induced on the pyrite surface and that it inhibited pyrite oxidation under acid conditions. The oxidation of pyrite by  $\text{H}_2\text{O}_2$  and NaOAC below pH 4 was inhibited by formation of an amorphous ferric hydroxide coating on the surface of pyrite, which most likely inhibited  $\text{H}_2\text{O}_2$  diffusion to the pyrite surface. This was consistent with the solubility of amorphous ferric hydroxide ( $\text{Fe}(\text{OH})_3$ ). Therefore inhibition of pyrite oxidation was caused by a pyrite coating including ferric hydroxide and silicate. Such pyrite coating may decrease oxidation via two mechanisms: (1) eliminating  $\text{Fe}^{3+}$  from the system by adsorption onto silica, (2) the coating may act as a physical barrier to  $\text{H}_2\text{O}_2$  and  $\text{Fe}^{3+}$ , inhibiting their diffusion to the pyrite surface.

Georgopoulou et al. (1995) studied the feasibility and cost of creating an iron-phosphate coating on pyrrhotite to prevent oxidation. They revealed that the iron-phosphate coating controlled the oxidation process of pyrrhotite under functional condition by stabilizing pH at around 4 (pH at which the oxidation rate is at a minimum) and by considerably reducing iron generation. Hydrogen peroxide ( $\text{H}_2\text{O}_2$ ) is necessary in the coating solution and its functional concentration depends on the experiment scale. The following two sets of coating conditions were carried out in comparison: (1) micro-columns, 4 g of pyrrhotite, 0.2 M  $\text{H}_2\text{O}_2$ , 0.2 M NaAC and 0.2 M  $\text{KH}_2\text{PO}_4$ . (2) large columns, 100 g of pyrrhotite, 0.01 M  $\text{H}_2\text{O}_2$ , 0.2 M NaAC and 0.2 M  $\text{KH}_2\text{PO}_4$ . It was also observed that a combination of pyrrhotite coating and phosphate rock around the coated particles behaves better than coating alone. The cost for applying the coating technique depends mostly on the concentration of the reagents but is in the order of a few dollars per tonne of tailings containing about 30% pyrrhotite. This cost is lower than the cost of conventional neutralization with limestone. Therefore iron-phosphate coating seems to be a promising technology for the abatement of AMD generation by pyrrhotite tailings. It has a potential to be applied as a long term solution alone or to be coupled with another prevention method.

Nyavor and Egiebor (1995) investigated control of pyrite oxidation by phosphate coating. They reported that chemical oxidation of pyrite can be reduced significantly by phosphate coating. The phosphate treatment has been shown to form an iron phosphate coating on pyrite particles, thereby preventing the ingress of oxidants into the pyrite matrix, which reduces the rate of pyrite oxidation. The application of low and high temperature phosphating of pyrite to control its rate of oxidation was investigated. It was also observed that although thicker coatings are formed using high phosphating temperature, these thicker coatings do not significantly improve the protection of the pyrite over thinner coatings formed under ambient condition. Using 60 °C and 200 psi oxygen pressure, about 480 minutes of reaction time in the autoclave corresponded to about 81 days in the accelerated oxidation column. The use of an autoclave for testing the stability of treated pyrite particles has been shown to be a more reliable and faster alternative to the conventional column oxidation test.



สถาบันวิทยบริการ  
จุฬาลงกรณ์มหาวิทยาลัย

## CHAPTER III

### METHODOLOGY

#### 3.1 Materials

The main materials used in this experimental study included as follows:

3.1.1 Pyrite ( $\text{FeS}_2$ ) in this study was obtained from the gold mine in Amphoe Thap Khlo, Changwat Phichit (Akara Mining Limited), northern Thailand.

3.1.2 Silica sand, 1-2 mm grain size

3.1.3 Chemical reagents:

- Hydrochloric acid (HCl)
- Hydrogen peroxide ( $\text{H}_2\text{O}_2$ )
- Sodium acetate (NaAc)
- Potassium hydrogen phosphate ( $\text{KH}_2\text{PO}_4$ )
- Calcium hydroxide ( $\text{Ca}(\text{OH})_2$ )

3.1.4 Glassware: vials and columns with 10 mm and 50 mm of diameter.

#### 3.2 Experiment Procedures

Experimental procedure of coating iron-phosphate on the surface of pyrite was carried out in batches in the laboratory of the National Research Center for Environmental and Hazardous Waste Management (NRC-EHWM) by following the process as described by Evangelou and Huang (1992).

In order to verify the feasibility of establishing an iron phosphate coating on pyrite, experiments were carried out under laboratory conditions. The methods in this study were divided into three main parts as below:

### 3.2.1 Pyrite Sample Preparation

Sufficient pyrite samples obtained from the gold mine were crushed by hammer and were sieved to retain the pyrite at the grain size between mesh number 20 and 40 or equate to between 425  $\mu\text{m}$  to 850  $\mu\text{m}$ . The prepared pyrite samples (Figure 3.1a) were then mixed with clean sand 1-2 mm in diameter (Figure 3.1b) in the ratio of 1 to 4. Mixing of sand in pyrite promotes the hydraulic conductivity to the system and hence the completion in reaction within the system expected from the experiment.



Figure 3.1 Pyrite samples (425 - 850  $\mu\text{m}$ ) and sand (1 - 2 mm) before coating.

### 3.2.2 Coating Process

The optimum conditions of the coating process were investigated by varying the concentrations of coating solutions ( $\text{H}_2\text{O}_2$ ,  $\text{KH}_2\text{PO}_4$  and  $\text{NaAc}$ ) and different contact times of the coating solution and the mixed pyrite and sand. The whole coating processes were divided into five steps as performed by Evangelou and Huang (1992)

for the pyrite coating. This process was conducted in batches containing coating solutions at different concentrations of  $\text{KH}_2\text{PO}_4$  and  $\text{H}_2\text{O}_2$  as mention earlier.

The steps of the coating process are the following: (as shown in Figure 3.2)

#### 3.2.2.1 Loading

The mixture of prepared pyrite and sand for 10 g at ratio of 1 to 4 respectively was loaded in the glass vials as a total of thirty vials.

#### 3.2.2.2 Surface preconditioning

The mixture in each vial was treated by 15 ml of 2 M hydrochloric acid solution (HCl solution) with constantly and regularly agitation for a period of length of time. The vials were agitated to allow the contact of the chemical and the pyrite samples in order to clean the sample surface. The spent hydrochloric solution was then discharged from the vials. Any oxide or hydroxide component that might have formed on the surface of pyrite would be set free to allow the pyrite to be ready for further reaction.

#### 3.2.2.3 Rinsing

The samples of preconditioning pyrite were rinsed repeatedly by distilled water until the pH value of the rinsed solution was raised to about 5. The pH value ranging form 5 to 6 is allowed to iron - phosphate precipitation on the pyrite particles (Georgopoulou et al., 1995).

#### 3.2.2.4 Coating

Five coating solutions, A, B, C, D and E were prepared by mixing of varying concentration of  $\text{KH}_2\text{PO}_4$  and  $\text{H}_2\text{O}_2$  with constant concentration of NaAc. Specification of each of the above mentioned solution was described in detail below:

Solution A = 0.2 M  $\text{KH}_2\text{PO}_4$  + 0.2 M  $\text{H}_2\text{O}_2$  + 0.2 M NaAc

Solution B = 0.3 M  $\text{KH}_2\text{PO}_4$  + 0.2 M  $\text{H}_2\text{O}_2$  + 0.2 M NaAc

Solution C = 0.1 M  $\text{KH}_2\text{PO}_4$  + 0.2 M  $\text{H}_2\text{O}_2$  + 0.2 M NaAc

Solution D = 0.2 M  $\text{KH}_2\text{PO}_4$  + 0.33 M  $\text{H}_2\text{O}_2$  + 0.2 M NaAc

Solution E = 0.2 M  $\text{KH}_2\text{PO}_4$  + 0.01 M  $\text{H}_2\text{O}_2$  + 0.2 M NaAc

A totally thirty experimental samples of 10 grams each of the prepared pyrite plus sand in vials were added to be reacted by 15 ml of the coating solution. These were six vials for each type of coating solution, which represented six contact times between the pyrite mineral and the coating solution. These six different contact times for the reaction to take place which are (a) instantaneous reaction which would take about 0-1 minute, (b) 10 minutes, (c) 20 minutes, (d) 30 minutes, (e) 40 minutes, (f) 50 minutes and (g) 60 minutes. The pyrite sample and the coating solution were allowed to react effectively by agitating motion in a shaker. The solutions tapped from the vials after reaction of forming coating substance on pyrite surface at different duration was brought to measure for the pH value and the remaining phosphate concentration. Preferably, these solutions were reserved in glassware bottles for phosphate determination because phosphate may be adsorbed onto the walls of plastic bottles (Eaton, Clesceri and Greenberg, 1995).

Chemically, hydrogen peroxide ( $\text{H}_2\text{O}_2$ ) in the coating solution strongly oxidizes the pyrite at the surface to produce ferric ion ( $\text{Fe}^{3+}$ ) to be ready to react with potassium hydrogen phosphate ( $\text{KH}_2\text{PO}_4$ ) to form surface coating substance of iron phosphate ( $\text{FePO}_4$ ). Sodium acetate (NaAc) is an important reagent in this coating process by playing a role as a buffer reagent.

#### 3.2.2.5 Stabilization

Add 20 ml of 800 mg/l concentration of calcium hydroxide solution ( $\text{Ca}(\text{OH})_2$ ) into the iron phosphate coated pyrite. Agitate the mixture of coated pyrite -  $\text{Ca}(\text{OH})_2$  in the shaker for ten minutes. This procedure would firmly stabilize the existence of the coated substance. Spent  $\text{Ca}(\text{OH})_2$  solution was subsequently discharged.

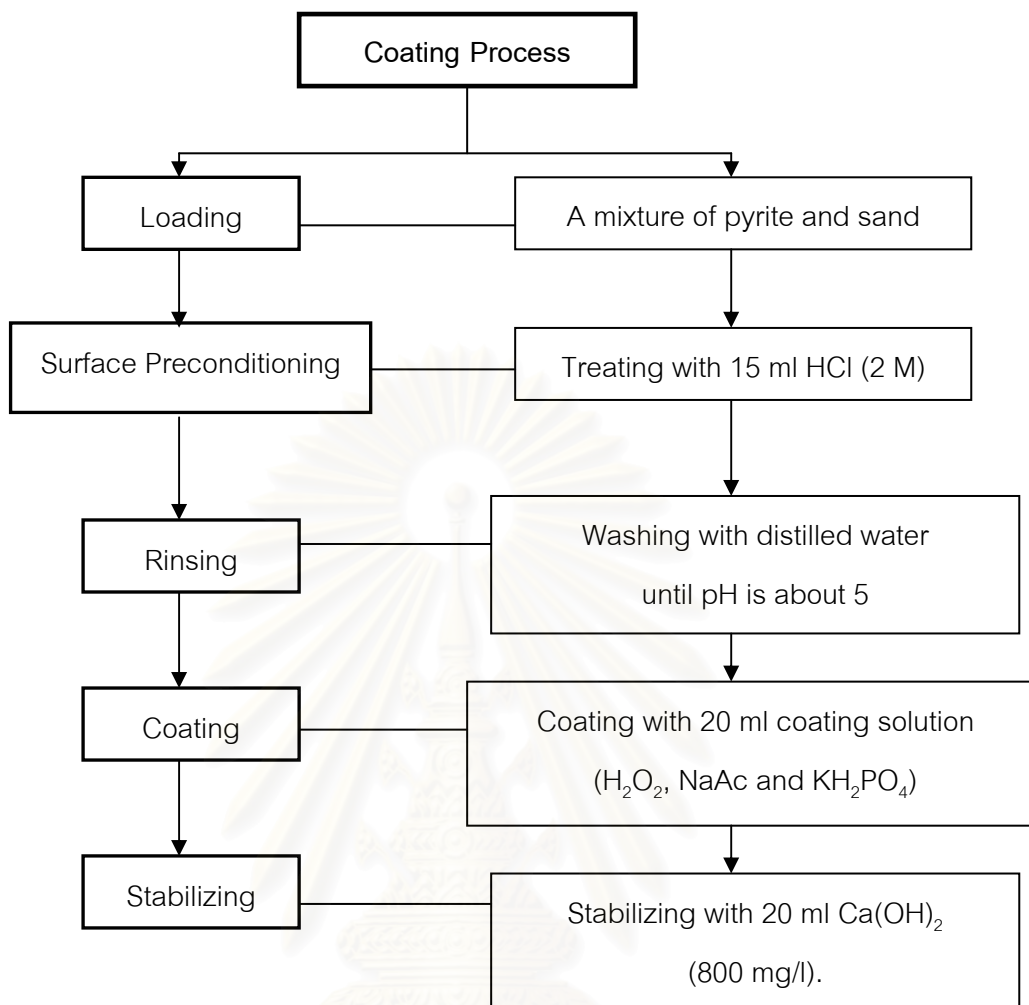


Figure 3.2 The simplified flow chart exhibiting the coating process (Evangelou and Huang, 1992).

### 3.2.3 Leaching Study

The effectiveness of the coated substance,  $\text{FePO}_4$ , to prevent the underlying pyrite to be oxidized to generate acid mine drainage (AMD) was determined by leaching test method. The coated pyrite was fed intermittently by hydrogen peroxide solution ( $\text{H}_2\text{O}_2$ ) to simulate the oxidation process in natural hydraulic cycles.  $\text{H}_2\text{O}_2$  reagent was chosen for leaching study because it creates an extremely oxidizing environment. In the  $\text{H}_2\text{O}_2$  solution, the concentration of dissolved oxygen is much higher than that occurs

naturally (Georgopoulou et al., 1995). The sequences of the leaching study are as the following and as shown in Figure 3.3).

- Air dry each sample of the mixture of pyrite and sand after the preceding coating process.
- Load 10 g of each of the mixture of pyrite and sand samples into the glass columns of 10 mm in diameter and 400 mm in length which underlain with glass wool to filter the solid from loss through the bottom of the column (see Figure 3.4).
- Leach the samples with a series of steps. 20 ml of 0.145 M hydrogen peroxide ( $H_2O_2$ ) solution was fed in each step for a period of 60 minutes. Therefore, the series of time is  $t = 0, 60, 120, 180, 240, 300, 360$  minutes. This step was designed by putting the solution into the column and then waiting for this solution flow through the column until the final drop of leachate was collected. In the next 60 minute, the  $H_2O_2$  solution was put into the column again and the leachate was then collected. This leaching process was continued until 360 minutes.
- Leachates from each of the leaching test were collected in plastic bottles for subsequently analyzing of the released iron concentration and for the pH value.

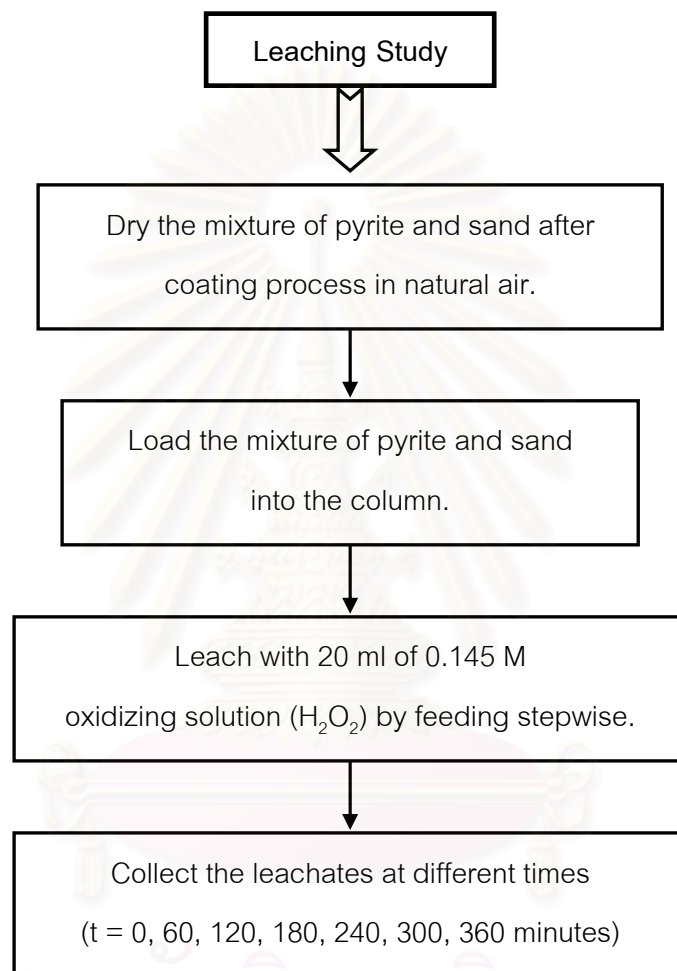


Figure 3.3 Simplified flow chart illustrating the steps of leaching study.



Figure 3.4 Leaching test in column with 10 mm of diameter x 400 mm long.

### 3.3 Analysis Methods

After coating process and leaching study, solutions collected from coating process and leachates collected from leaching test at different times were analyzed for determining the optimum condition of creating an iron-phosphate coating on pyrite surface. These chemicals analysis were conducted for two parts of the experiments; spent solution from coating and leachate from leaching study. The detail is as follows (see also Figure 3.5):

- Spent solution from coating process

Solutions collected at different times were analyzed for pH using PHM 83 Autocal pH meter and for phosphate concentration analyzed by ascorbic acid method. In addition, the coated pyrite which was separated from the mixture of pyrite and sand after coating process and non-coated pyrite samples was examined by Electron Probe Micro-Analyzer (EPMA) to identify the chemicals composition on the surface for quantitative analysis.

- Leachate

Leachates from the leaching test were measured for pH using PHM 83 Autocal pH meter and analyzed for total iron released by Flame Atomic Absorption Spectrometry (AAS) to examine the resistance of the coated pyrite. Basically, pH value, total iron and sulfate are the three primary parameters indicating the potential of acid mine drainage (AMD) and pyrite oxidation (Adams et al., 1994).

### 3.3.1 Ascorbic Acid Method

This method is a standard method for the examination of the phosphate concentration in water and wastewater. Thus it was selected for analyzing the phosphate after coating process in this study. In principle, ammonium molybdate and potassium antimonyl tartrate react in acid medium with orthophosphate to form a heteropoly acid, phosphomolybdic acid, that is reduced to intensely colored molybdenum blue by ascorbic acid. The steps of phosphate determination are the following: (Eaton, Clesceri and Greenberg, 1995).

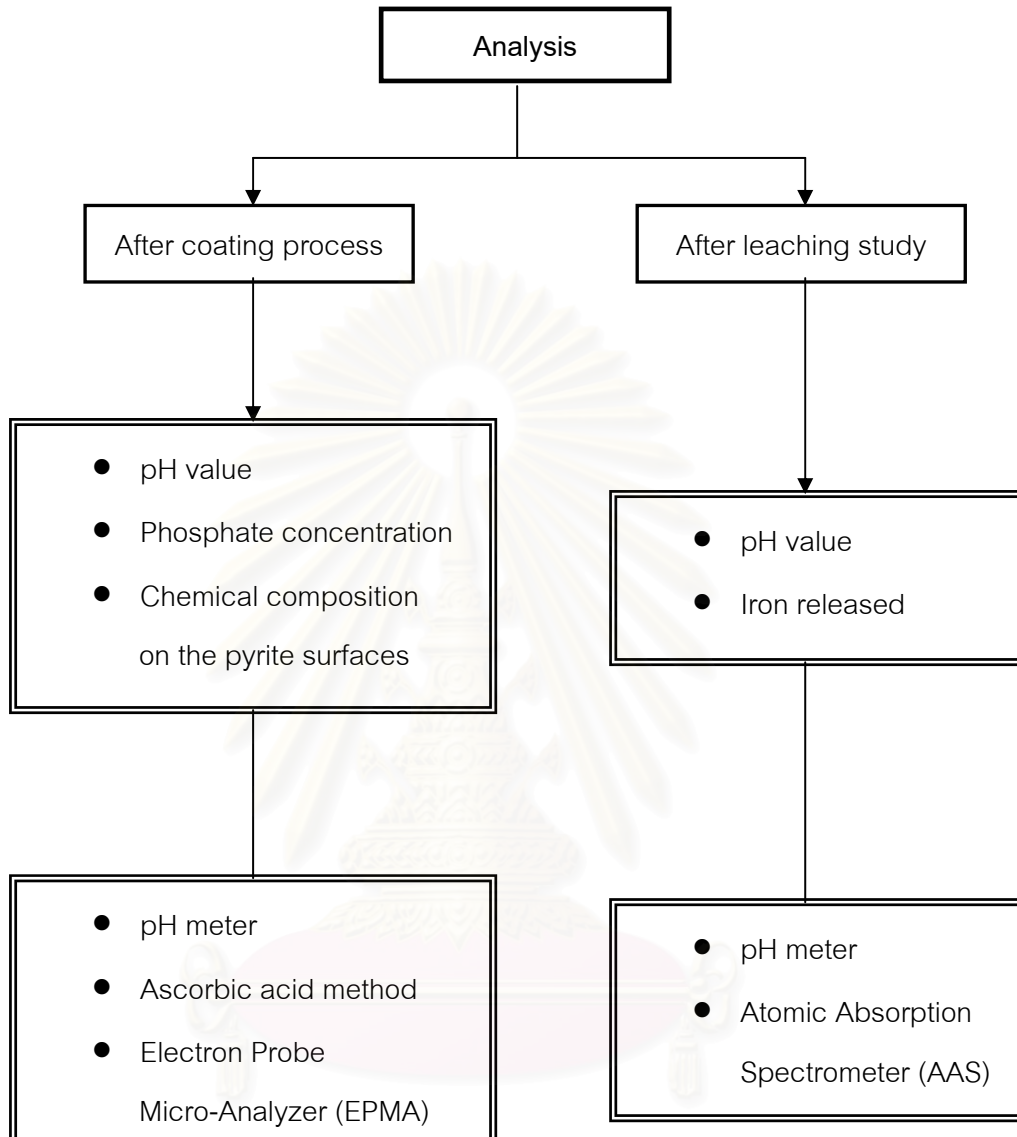


Figure 3.5 Flow chart displaying the analysis procedures.

### 3.3.1.1 Reagents preparation

The reagents used in this analysis are shown as below:

- Sulfuric acid ( $\text{H}_2\text{SO}_4$ ) 5 N: Dilute 70 ml of conc.  $\text{H}_2\text{SO}_4$  to 500 ml with distilled water.

- Potassium antimonyl tartrate solution: Dissolve 1.3715 g of  $K(SbO)C_4H_4O_6 \cdot 1/2H_2O$  in 400 ml distilled water in a 500 ml volumetric flask and dilute to volume. Store in a glass – stoppered bottle.
- Ammonium molybdate solution: Dissolve 20 g of  $(NH_4)_6Mo_7O_{24} \cdot 4H_2O$  in 500 ml distilled water. Store in a glass – stoppered bottle.
- Ascorbic acid 0.1 M: Dissolved 1.76 g ascorbic acid in 100 ml distilled water. The solution is stable for about 1 week at 4°C.
- Combined reagent: Mix the above reagents in the following proportions for 100 ml of the combined reagent: 50 ml of 5 N sulfuric acid, 5 ml of potassium antimonyl tartrate solution, 15 ml of ammonium molybdate solution and 30 ml of ascorbic acid solution. Mix after addition of each reagent and allow all reagents to reach room temperature before they are mixed. The combined reagent is stable for four hours.
- Stock phosphate solution: Dissolve in distilled water 219.5 mg of anhydrous  $KH_2PO_4$  and dilute to 1,000 ml (1 ml = 50 µg P).
- Standard phosphate solution: Dilute 50 ml of stock phosphate solution to 1,000 ml with distilled water (1 ml = 2.5 µg P).

### 3.3.1.2 Procedure

The procedures are to achieve in this method as below:

- Digestion: Use 50 ml or a suitable portion of mixed sample. Then, add 1 ml of 5 N  $H_2SO_4$  solution and either 0.4 g solid ammonium persulfate ( $(NH_4)_2S_2O_8$ ) or 0.5 g solid potassium persulfate ( $K_2S_2O_8$ ). Boil gently on a preheated hot plate for 30 to 40 minutes or until a final volume of 10 ml is reached. And cool, dilute to 30 ml with distilled water. Add 0.05 ml (1 drop) phenolphthalein indicator solution and neutralize to a faint pink color with 6 N NaOH. Then, add 5 N  $H_2SO_4$  solutions dropwise to just discharge the color. Finally, make up volume to 50 ml with distilled water.

Because phosphorus may occur in combination with organic matter, a digestion method to determine total phosphorus must be able to oxidize organic matter effectively to released phosphorus as orthophosphate. Generally, the simplest method is persulfate oxidation technique. It is recommended that this method be checked against

one or more of the more drastic digestion technique and be adopted if identical recoveries are obtained.

- Treatment of sample: Use 50 ml of the solution samples into 125 ml erlenmeyer flask. Then, add 8 ml of combined reagent and mix thoroughly. After at least 10 minutes but no more than 30 minutes, measure absorbance of each sample at 880 nm by using reagent blank as the reference solution.

- Preparation of calibration curve: Prepare individual calibration curves from a series six standards of phosphate concentration that are 0.05, 0.1, 0.2, 0.3, 0.4 and 0.5 mg/l. UV-Spectrophotometer is the apparatus using in this procedure. Use a distilled water blank with the combined reagent to make photometric readings for the calibration curve. Plot absorbance and phosphate concentration to provide a straight line passing through the origin.

- Calculate phosphate concentration from the relationship graph between absorbance value (Y – axis) and phosphate concentration (X – axis) with the linear equation ( $y = mx + c$ ).

### 3.3.2 Metals by Flame Atomic Absorption Spectrometry

This apparatus was used for determining iron released after leaching study. Because requirements for determining metals by atomic absorption spectrometry vary with metal or concentration to be considered, determination of iron can be gathered into Metals by Flame Atomic Absorption Spectrometry.

In principle, a sample is aspirated into a flame and atomized. A light beam is directed through the flame, into monochromator, and onto a detector that measures the amount of light absorbed by the atomized element in the flame. For some metals, atomic absorption exhibits superior sensitivity over flame emission. Because each metal has its own characteristic absorption wavelength, a source lamp composed of that element is used, this makes the method relatively free from spectral or radiation interferences. The amount of energy at the characteristic wavelength absorbed in the flame is proportional to the concentration of the element in the sample over a limited concentration range.

Most atomic absorption instruments also are equipped for operation in an emission mode (Eaton, Clesceri and Greenberg, 1995).

The sensitivity of flame atomic absorption spectrometry is defined as the metal concentration that produces an absorption of 1% (an absorbance of approximately 0.0044). The instrument detection limit is defined here as the concentration that produces absorption equivalent to twice the magnitude of the background fluctuation.

### 3.3.2.1 Procedure

The procedures are exhibited as below:

- Treatment of sample solution: Add 0.05 ml (1 drop) of conc. nitric acid ( $\text{HNO}_3$ ) into the sample solutions. Then, agitate the solutions.
- Preparation of calibration curve: Prepare standard solutions of the iron in concentration of 1, 2, 4, 10 and 20 mg/l. Run blank as the reference solution. Standard solutions and sample solutions were aspirated into atomic absorption spectrometer. It provides the relationship graph between absorbance (Y – axis) and iron concentration (X – axis) that can be calculated to quantity of iron released in sample solutions.

### 3.3.3 Electron Probe Micro Analyzer (EPMA)

The equipment was used for examining the chemical composition on the surface of the coated pyrite after coating process and non-coated pyrite. In principle, EPMA is basically operated by bombarding a micro - volume of a sample with a focused electron beam (typical energy = 5 - 30 keV) and collecting the X - ray photons thereby induced and emitted by the various elemental species. Because the wavelengths of these X-rays are characteristic of the emitting species, the sample composition can be easily identified by recording WDS spectra (Wavelength Dispersive Spectroscopy). Figure 3.6 shows the effects produced by electron bombardment of a material.

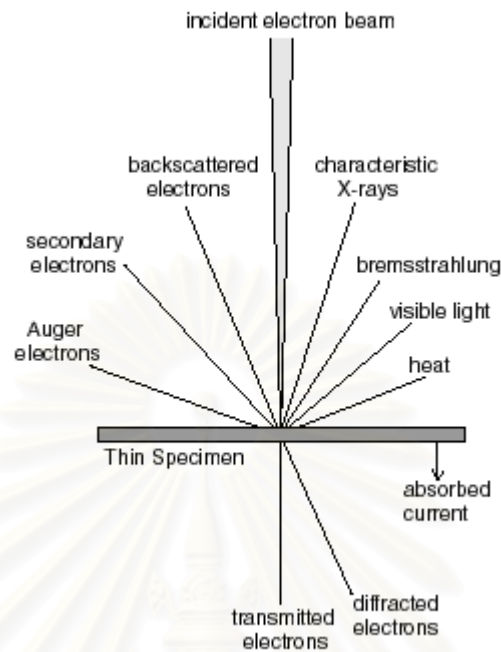


Figure 3.6 Effects produced by electron bombardment of a material  
(Available from: [www.cameca.fr](http://www.cameca.fr)).

### 3.3.3.1 Effects of electron bombardment

Electron bombardment of a sample is unique to microprobe analysis and produces a large number of effects from the target material (Figure 3.6). The incident electrons interact with specimen atoms and are significantly scattered by them. Most of the energy of an electron beam will eventually end up heating the sample, however, before the electrons come to rest, they undergo two types of scattering: elastic and inelastic.

In elastic scattering, the electron path changes, but its kinetic energy and velocity remain essentially constant due to large differences between the mass of the electron and nucleus. This process is known as electron backscattering.

In inelastic scattering, the path of the incident electron is only slightly disturbed, but energy is lost through interactions with the orbital electrons of the atoms

in the specimen. Inelastic interactions produce diverse effect including heating, visible light fluorescence, continuum radiation (or braking radiation), characteristic of X-ray radiation, secondary electrons and ejection of outer shell electrons.

X - rays are electromagnetic radiation. All X - rays represent a very energetic portion of the electromagnetic spectrum (Figure 3.7) and have short wavelengths of about 0.1 to 100 angstroms (Å). They are bounded by ultraviolet light at long wavelengths and gamma rays at short wavelengths. X - rays in the range from 50 to 100 angstroms are termed soft X - rays because they have lower energies and are easily absorbed.

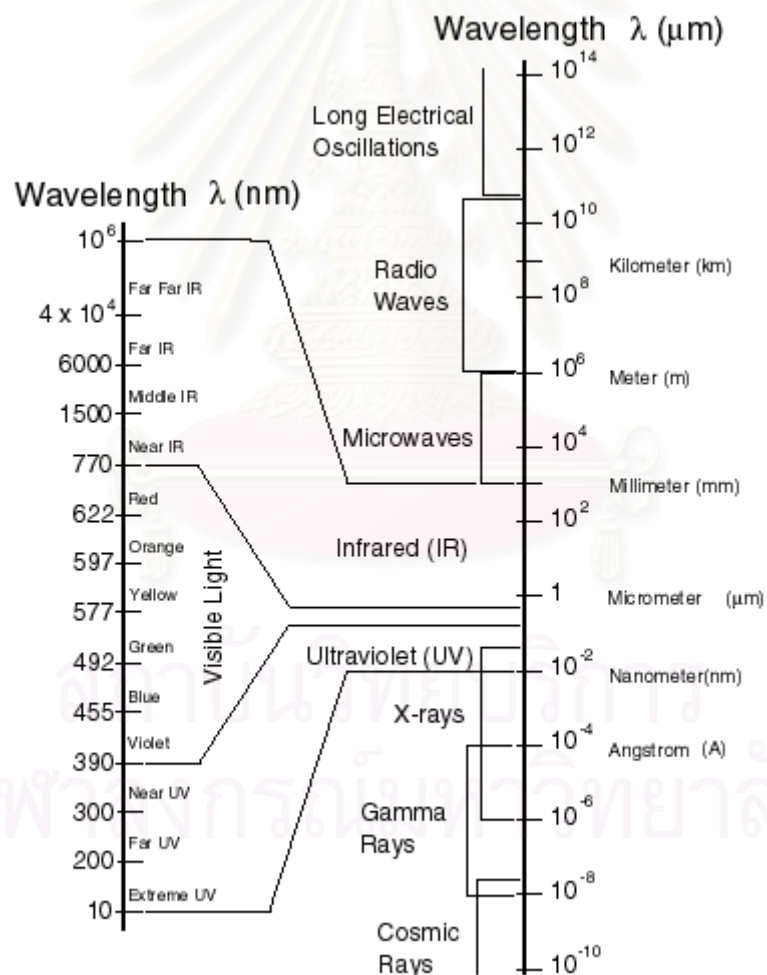


Figure 3.7 Electromagnetic spectrum (Available from [www.cameca.fr](http://www.cameca.fr)).

### 3.3.3.2 Procedure

The procedures are exposed as below:

- Preparation of samples: Both the coated pyrite and non-coated pyrite samples were prepared into the block of resin by using resin mixed with hardener. Then, samples would be dried in natural air. After that, the samples were coated by carbon coating process for analyzing the chemical composition on the surface of pyrite samples.
- Operation with EPMA: The prepared pyrite samples were loaded into the block by which six samples can be contained into one block. Then, this block with the samples was carried into the hole of EPMA apparatus (Figure 3.8) for quantitative analysis.



**Figure 3.8** Electron Probe Micro Analyzer (EPMA) used for analyzing the chemical composition on the pyrite surface (Available from: [www.hardcoatings.ac.at](http://www.hardcoatings.ac.at)).

### 3.4 Application with the Soil Mining Wastes

In order to estimate the effectiveness of the optimum coating solution in the pyrite coating preventing pyrite oxidation in real situation, these approach was carried out in column with 50 mm of diameter and 500 mm long containing soil mining wastes from the Banpu Public Company Limited Coal Mine, Amphoe Lee, Changwat Lumphun. And this step was followed by the coating process and leaching study that described previously. The main differences are the following (see also Figure 3.9):

- Soil mining wastes were crushed by rubber hammer in order to obtain the grain size is less than 1 cm. Then they were mixed with gravel in ratio 3 : 1 (150 g of soil mining waste : 50 g of gravel) for increasing the flow of solution in the soil sample.
- The mixtures of soil sample and gravel were loaded into the columns, 50 mm of diameter and 500 mm long, with stopcocks for coating process and leaching study. Glass wool was also placed at the bottom of column as a filter to avoid solid loss through the bottom of the column
- In the coating process, leaching with the coating solution 200 ml in the concentration of 0.2 M  $\text{KH}_2\text{PO}_4$  + 0.2 M  $\text{H}_2\text{O}_2$  + 0.2 M NaAc were carried out by putting the coating solution into the column while a stopcock was opened and collected the leachate until no solution dropped to the beaker. The leachate was then measured for pH value.
- In the leaching study, both the soil samples after coating process and soil sample without coating were leached with 100 ml of 0.2 M oxidizing solution ( $\text{H}_2\text{O}_2$ ) by stepwise feeding at different times (every 24 hours). By which the  $\text{H}_2\text{O}_2$  solution was put into the column with opened stopcock and then left this column for 24 hours until leachate was not dropped in beaker. After that, putting the solution was performed again and collected the leachate. This leaching process was conducted until 120 hours. Leachate was gathered for measuring the pH value and analyzing the iron released.

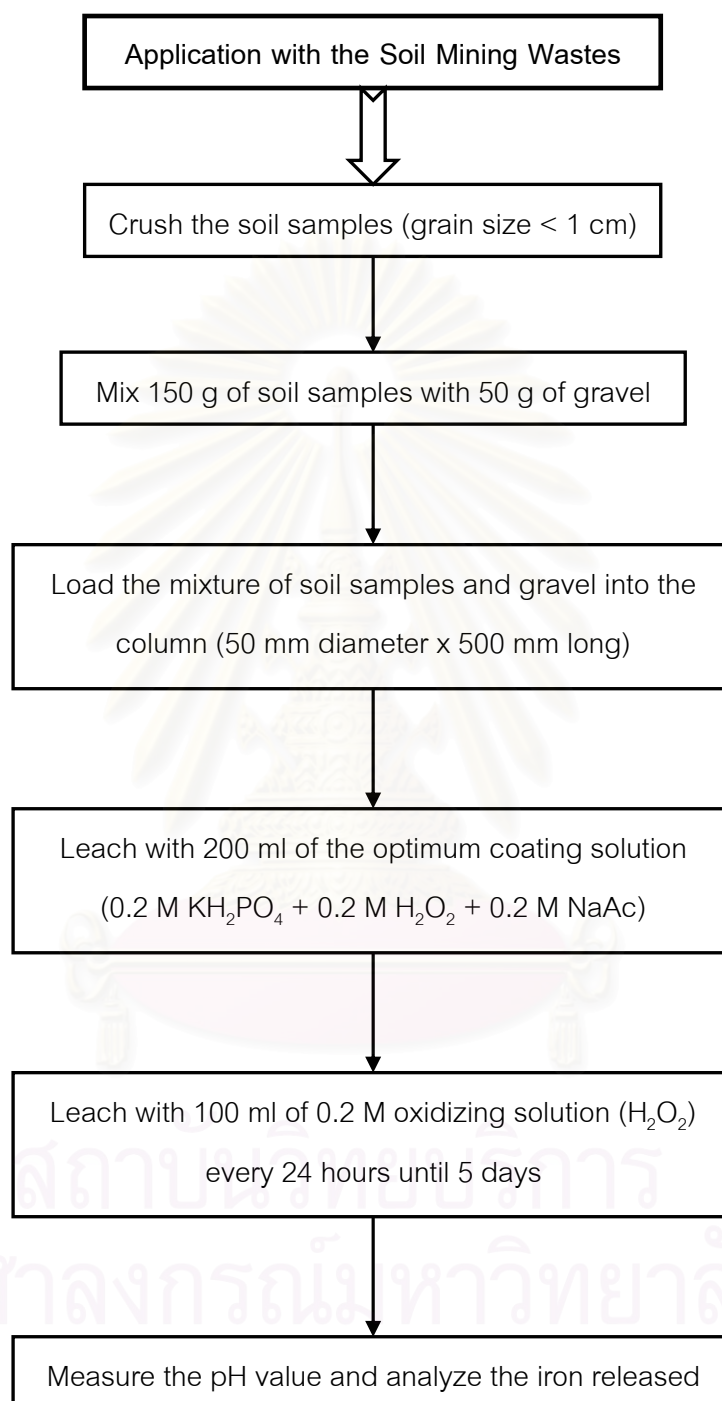


Figure 3.9 Simplified flow chart showing the steps of application with soil mining wastes.



Figure 3.10 Application with the soil mining wastes studied in column with 50 mm of diameter x 500 mm long.

## CHAPTER IV

### RESULTS AND DISCUSSION

#### 4.1 Iron-phosphate Coating on Pyrite Surfaces Using Various Coating Solutions

A mixture of chemical reagents used to stimulate the surface of pyrite mineral to be ready to react to form iron-phosphate ( $\text{FePO}_4$ ) coating is composed of potassium hydrogen phosphate ( $\text{KH}_2\text{PO}_4$ ), hydrogen peroxide ( $\text{H}_2\text{O}_2$ ) and sodium acetate (NaAc). Regarding to the functioning effects on coating process of these reagents,  $\text{KH}_2\text{PO}_4$  provides phosphate for coating,  $\text{H}_2\text{O}_2$  oxidizes pyrite to produce ferric ion ( $\text{Fe}^{3+}$ ) to react with  $\text{KH}_2\text{PO}_4$  to form iron-phosphate ( $\text{FePO}_4$ ) and NaAc is a buffering agent.

In this study, five mixtures of coating solution were prepared by varying in the amount of  $\text{KH}_2\text{PO}_4$  and  $\text{H}_2\text{O}_2$  with constant NaAc. They were listed as the following:

Solution A = 0.2 M  $\text{KH}_2\text{PO}_4$  + 0.2 M  $\text{H}_2\text{O}_2$  + 0.2 M NaAc

Solution B = 0.3 M  $\text{KH}_2\text{PO}_4$  + 0.2 M  $\text{H}_2\text{O}_2$  + 0.2 M NaAc

Solution C = 0.1 M  $\text{KH}_2\text{PO}_4$  + 0.2 M  $\text{H}_2\text{O}_2$  + 0.2 M NaAc

Solution D = 0.2 M  $\text{KH}_2\text{PO}_4$  + 0.33 M  $\text{H}_2\text{O}_2$  + 0.2 M NaAc

Solution E = 0.2 M  $\text{KH}_2\text{PO}_4$  + 0.01 M  $\text{H}_2\text{O}_2$  + 0.2 M NaAc

Different mixture of coating solutions were designed to determine the quantity and the quality of coating material of iron-phosphate ( $\text{FePO}_4$ ) on the surface of the pyritic mineral. It is, therefore, essential to quantify the optimum condition of the formation of the coating material and also the resistance of this coating material in inhibiting oxidation process to develop at the surface of these pyrites underneath.

Spent solutions after being used for the reaction in the coating process at various contact times would be collected to the measure for the value of pH and phosphate concentration in order to obtain the acid-base condition and the amount of phosphate used and remained in the solution.

In Table 4.1 and Figure 4.1, it was obvious that the pH values of the remaining solution of these five varying coating solutions measured after react with pyrite were quite uniform. The pH values in the solutions ranged from 4.88 to 5.80. This was owing to 0.2 M of sodium acetate (NaAc) admixed in these coating solutions buffered the pH of the coating solutions at the range of 5 to 6 (Georgopoulou et al., 1995).

**Table 4.1** pH in solution remained after treating with varying coating solutions at different contact times.

Time (minute)	pH				
	Solution A	Solution B	Solution C	Solution D	Solution E
0	4.93	4.88	4.95	4.89	4.90
10	5.73	5.46	5.80	5.62	5.60
20	5.71	5.47	5.79	5.61	5.59
30	5.72	5.48	5.79	5.60	5.59
40	5.72	5.48	5.79	5.61	5.60
50	5.73	5.51	5.80	5.60	5.60
60	5.71	5.47	5.79	5.61	5.61

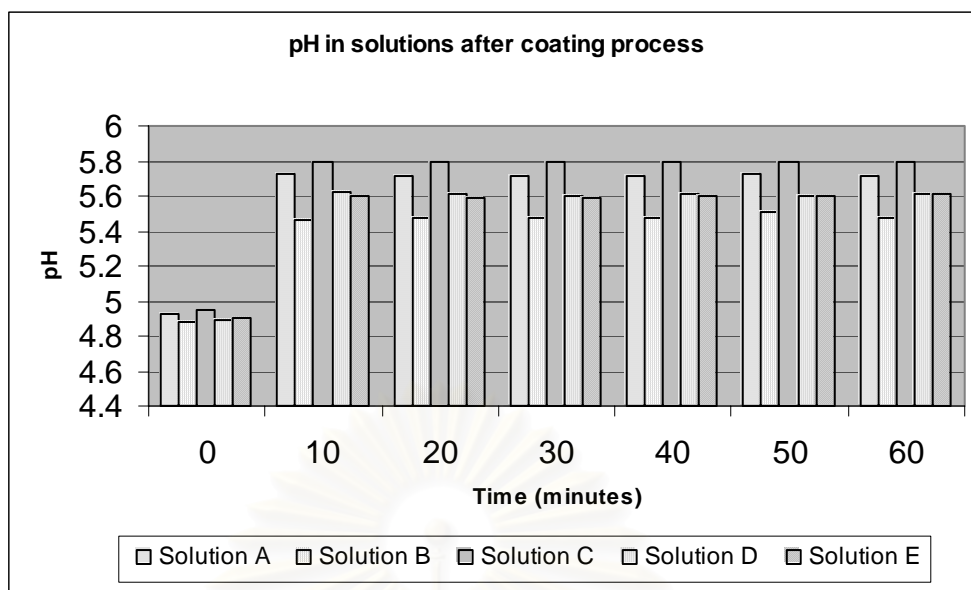


Figure 4.1 Trends of pH value measured after treating with various coating solutions at different contact times (at the time of  $t_0$  is the pH value after rinsing with distilled water before adding coating solution).

#### 4.1.1 Effect of potassium hydrogen phosphate ( $\text{KH}_2\text{PO}_4$ ) on creating an iron-phosphate coating

As potassium hydrogen phosphate ( $\text{KH}_2\text{PO}_4$ ) provides phosphate component to react with  $\text{Fe}^{3+}$  to form coating substance as described previously. Therefore, the remaining phosphate concentration in the coating solutions after the coating process is inevitably needed to be considered. In the experiment, the concentration of  $\text{KH}_2\text{PO}_4$  component in the coating solution was designed to be variable in order to determine the concentration effect on the formation of coating substance. Solution A, B and C are the subjects of this experiment and the solution A is referred to be the reference solution as described below:

Solution A = 0.2 M  $\text{KH}_2\text{PO}_4$  + 0.2 M  $\text{H}_2\text{O}_2$  + 0.2 M NaAc

Solution B = 0.3 M  $\text{KH}_2\text{PO}_4$  + 0.2 M  $\text{H}_2\text{O}_2$  + 0.2 M NaAc

Solution C = 0.1 M  $\text{KH}_2\text{PO}_4$  + 0.2 M  $\text{H}_2\text{O}_2$  + 0.2 M NaAc

According to the Table 4.2 and Figure 4.2, it was obviously observed that though the remaining phosphate content in coating solution B was the lowest when compared with remaining phosphate in coating solution A and C in terms of number, it was, however, insignificantly different when these number were shown in terms of ratio of the remaining to the original content. It is only apparent that the coating substance withdrawn from solution B to deposit on the surface of pyrite is better than from the solution A and C.

**Table 4.2** Phosphate remaining in solutions after treating with various coating solutions at different contact times.

Time (minute)	Phosphate (mg/l)				
	Solution A	Solution B	Solution C	Solution D	Solution E
10	10.625	0.717	7.007	0.722	6.737
20	9.750	0.497	6.770	0.840	7.670
30	10.075	0.725	7.577	1.177	7.132
40	10.275	0.745	8.082	5.547	9.872
50	9.625	0.730	8.410	5.642	9.375
60	10.375	0.610	7.635	0.900	10.770

สถาบันวิทยบริการ  
จุฬาลงกรณ์มหาวิทยาลัย

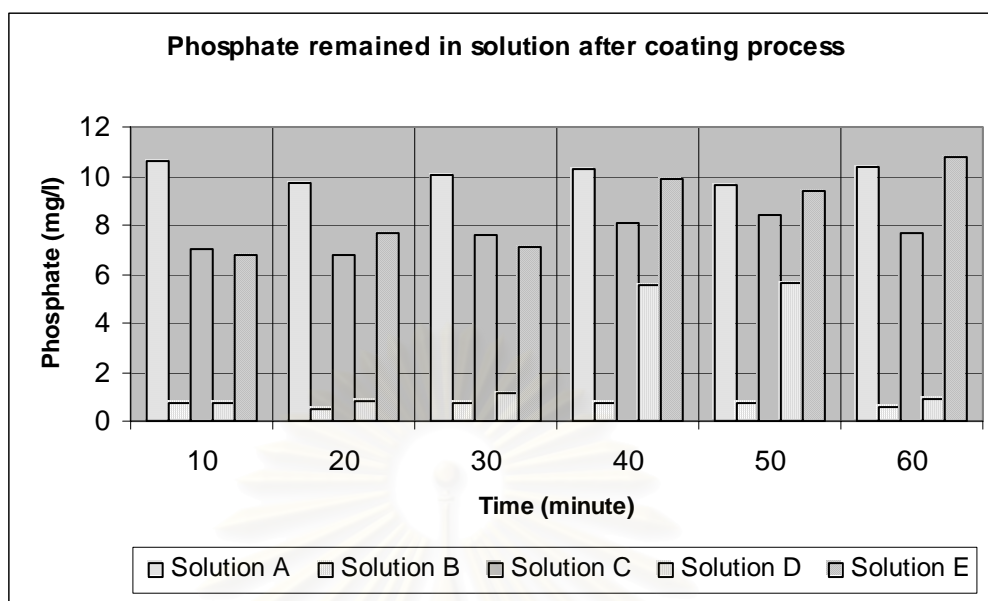


Figure 4.2 Variation of remaining phosphate concentration after treating with various coating solutions at different contact times.

#### 4.1.2 Effect of hydrogen peroxide (H<sub>2</sub>O<sub>2</sub>) on creating an iron-phosphate coating

Hydrogen peroxide (H<sub>2</sub>O<sub>2</sub>), a strong oxidizing reagent, oxidizes the pyrite surface to produce ferric ion (Fe<sup>3+</sup>) to be available to react with the phosphate reagents to form iron-phosphate (FePO<sub>4</sub>) as previously mentioned. By varying the concentration of H<sub>2</sub>O<sub>2</sub> in the coating solution, the amount of induced ferric iron on the pyrite surface is expected to vary accordingly hence the amount of phosphate concentration during coating process. Coating solution A, D and E are different only on their H<sub>2</sub>O<sub>2</sub> concentrations as shown below and solution A is designated as reference solution.

Solution A = 0.2 M KH<sub>2</sub>PO<sub>4</sub> + 0.2 M H<sub>2</sub>O<sub>2</sub> + 0.2 M NaAc

Solution D = 0.2 M KH<sub>2</sub>PO<sub>4</sub> + 0.33 M H<sub>2</sub>O<sub>2</sub> + 0.2 M NaAc

Solution E = 0.2 M KH<sub>2</sub>PO<sub>4</sub> + 0.01 M H<sub>2</sub>O<sub>2</sub> + 0.2 M NaAc

It is apparent from the Table 4.2 and Figure 4.2 that the remaining phosphate concentration in coating solution D was lower than those of the solutions A and E. Larger amount of  $H_2O_2$  causes higher oxidation rate hence higher amount of ferric iron ( $Fe^{3+}$ ) from pyrite surface to react with phosphate.

Moreover, it illustrated that concentration of remaining phosphate in solutions A, C and E after coating process were considerably higher than solutions B and D. Thus, treating pyrite with these, A, C and E coating solutions resulted in the lower quantity of phosphate consumed to form the coating substance whereas the possibility of phosphate consumption for surface coating in the solutions B and D was apparently better.

From these results of the coating experiment, the coating solution B could have been considered the optimum combination of reagents for the coating process by judging from the pH value and the lowest concentration of remaining phosphate. However, these results are still needed to be further justified by the results of leaching test.

## 4.2 Chemical Composition on the Surfaces of Coated Pyrite

EPMA (Electron Probe Micro-Analyzer) was employed to determine the chemical composition of the coated substance on the surface of the pyritic sample and for comparison the composition of the uncoated pyrite. Table 4.3 shows the mass content of FeO, SO<sub>3</sub>, P<sub>2</sub>O<sub>5</sub> and total oxides of other elements. The coated pyrite samples used in this study were selected presumably from the best coating output formed on the surface of pyrite from aforementioned experiment of each coating solution. However, the best coating sample precipitated on the surface of pyrite from solution A was not included in this Table due to some error in sample preparation process prior to the EPMA measurement.

Mass proportions of elemental oxides in Table 4.3 are converted into atomic proportion of elements in Table 4.4. It is observed clearly from Tables 4.3 and 4.4 that the contents of Fe and S components are extraordinary high while that of P was relatively low. It is believed that the majority of elements analyzed were derived from the ionization of pyrite under the coated stratum. However, the coated substance is not only formed as FePO<sub>4</sub> but it can also be free phosphate (PO<sub>4</sub><sup>3-</sup>) remained from coating process.

Relatively, the coated substance FePO<sub>4</sub> on the surface of pyrite formed from coating solutions B and E appear to be more effective than those formed from coating solutions C and D. However, atomic proportions in Table 4.4 clearly indicate highest P atom resulted from solution B.

Ultimately, the results of EPMA analysis can support the possibility of phosphate and iron used for coating in the forms of iron-phosphate (FePO<sub>4</sub>) on the pyrite surfaces after coating process.

From data in Table 4.3 (supplementary in appendix), it is observed that FeO and SO<sub>3</sub> compounds are major composition analyzed from the surface of coated pyrite and

the surface of non-coated pyrite reflecting majority of elements derived from the chemical formula of pyrite which is  $\text{FeS}_2$  (Klein and Hurlbut, 1999).  $\text{P}_2\text{O}_5$ , is relatively much smaller content than those of  $\text{FeO}$  and  $\text{SO}_3$  reflecting the smaller quantity of the phosphate deposited on the pyrite surface.

**Table 4.3** The average of mass proportion on pyrite surfaces analyzed using EPMA after coating with solutions B, C, D and E.

Sample	Mass Proportion (%)			
	FeO	SO <sub>3</sub>	P <sub>2</sub> O <sub>5</sub>	Other elements
Non-coated pyrite	61.83	136.78	0.00	0.37
B (t 20)	58.90	127.49	2.52	3.73
C (t 20)	60.40	130.26	1.62	2.40
D (t 10)	58.91	127.94	1.86	2.15
E (t 10)	61.10	131.47	2.51	3.05

**Table 4.4** The average of atomic proportion on pyrite surfaces after coating with solutions B, C, D and E.

Sample	Atomic Proportion				
	Fe	S	P	Fe : S	S : P
Non-coated pyrite	0.136	0.269	0.000	0.504	-
B (t20)	0.120	0.234	0.052	0.514	59.240
C (t20)	0.145	0.281	0.004	0.517	112.452
D (t10)	0.144	0.281	0.005	0.514	95.201
E (t10)	0.139	0.268	0.024	0.517	80.251

Table 4.4 shows atomic proportion of elements analyzed by EPMA from the surface of coated pyrite. It is illustrated by the atomic ratio of S : P that is the lowest content yielded from coated surface in sample B (t20). It could probably suggest that the coated substance on the surface of pyrite in sample B (t20) is relatively better than other samples.

Moreover, the coated pyrite samples were visualized under scanning electron microscope (SEM) in order to observe the morphology of the surface of non-coated pyrite (Figure 4.3) and iron-phosphate formation on the pyrite surfaces as shown in Figures 4.4 to 4.7.

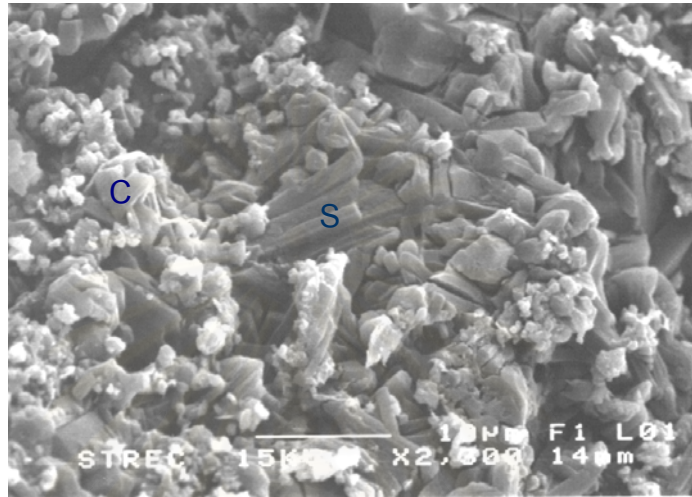


Figure 4.3 Secondary electron image of non-coated pyrite illustrating the surface of pyrite (C = clay mineral, S = pyrite).

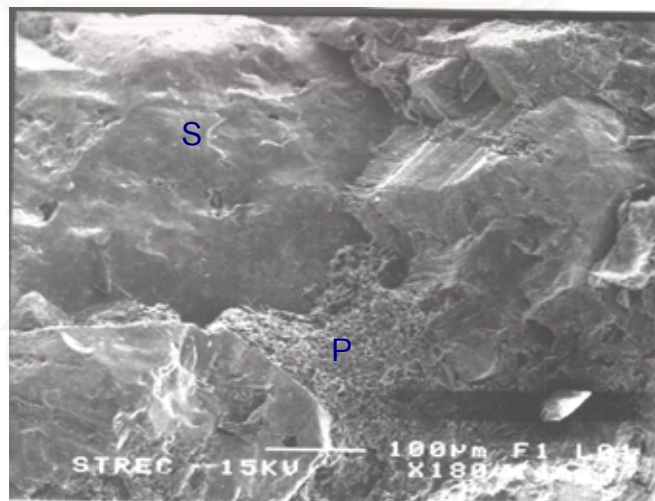


Figure 4.4 Secondary electron image of the pyrite coated by solution B illustrating iron-phosphate coating on the surface of pyrite (S = pyrite, P = iron-phosphate).

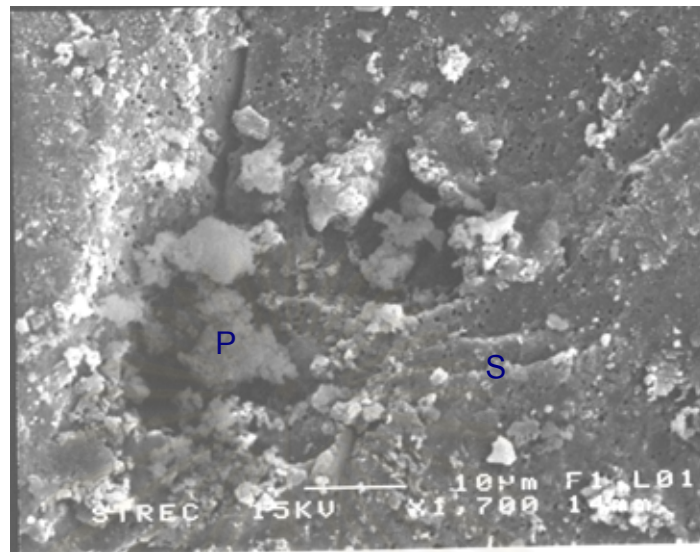


Figure 4.5 Secondary electron image of the coated pyrite using solution C illustrating iron-phosphate on the surface of pyrite (S = pyrite, P = iron-phosphate).

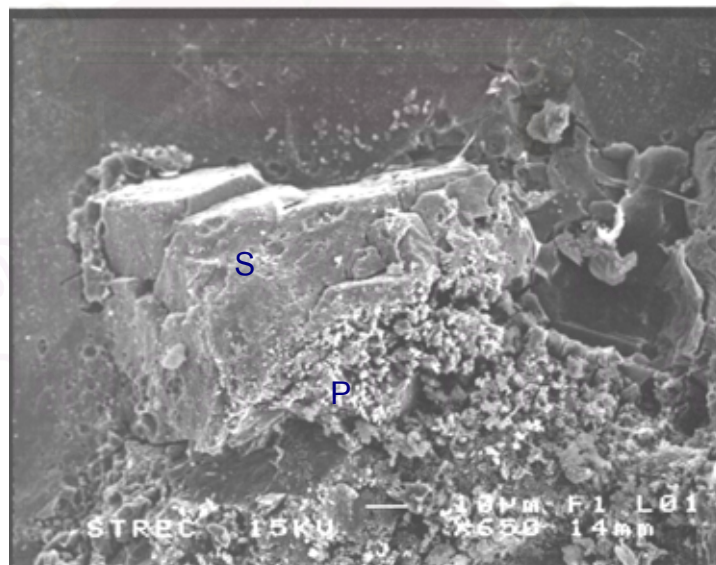


Figure 4.6 Secondary electron image of the coated pyrite using solution D illustrating iron-phosphate on the surface of pyrite (S = pyrite, P = iron-phosphate).

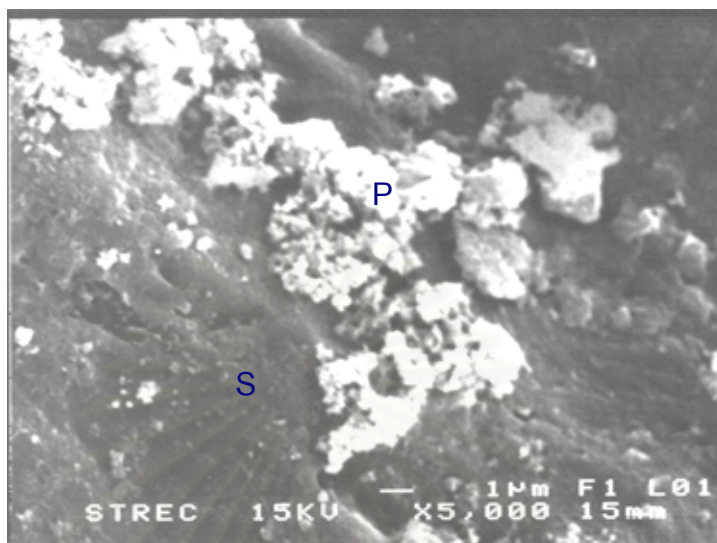


Figure 4.7 Secondary electron image of the coated pyrite using solution E illustrating iron-phosphate on the surface of pyrite (S = pyrite, P = iron-phosphate).

Figure 4.3 shows the surface of uncoated pyrite which is associated with some clay mineral. However, clay mineral is obviously disappeared on the surface of coated pyrite; it may be mostly washed during the coating process. On the other hand, irregular cloudy grains of iron-phosphate ( $\text{FePO}_4$ ) are increased on the coated surface as shown in Figures 4.4 to 4.7.

สถาบันวิทยบริการ  
จุฬาลงกรณ์มหาวิทยาลัย

### 4.3 Resistance of the Coated Pyrite to Oxidizing Condition

The coating  $\text{FePO}_4$  on pyrite surface prevents direct contact between pyrite oxygen ( $\text{O}_2$ ) and water ( $\text{H}_2\text{O}$ ) generating acid mine drainage (AMD). Hydrogen peroxide solution ( $\text{H}_2\text{O}_2$ ), a strong oxidizing reagent, has normally been used to test the leachability of the coating material and the capacity to penetrate and react with the underlying pyrite. Generation of acid activity measured in terms of pH value and dissolution of ferric ion concentration are two major indicators used for the leaching test and the resistance to oxidation capacity of the coated iron-phosphate ( $\text{FePO}_4$ ).

During leaching, total iron is a good index to characterize the pyrite oxidation rate since there is no phosphate to precipitate iron in the leachates. Also during leaching, free sulfur is formed instead of sulfide due to the higher oxidation potentials obtained in the presence of hydrogen peroxide ( $\text{H}_2\text{O}_2$ ) (Georgopoulou et al., 1995).

Generally, the concentration of  $\text{H}_2\text{O}_2$  solution used for the leaching test in most experiments is ranging from 0.017 M to 0.2 M (Georgopoulou et al., 1995). It was, however, decided to use the concentration of 0.145 M  $\text{H}_2\text{O}_2$  solution for the experiment in this study as suggested by Zhang and Evangelou (1998).

Two  $\text{FePO}_4$  coated pyrites were selected from each coating solution in Table 4.2, the minimum coated samples and the maximum coated samples. The minimum coated sample was the one with maximum phosphate concentration remained in solution of each coating solution such as A (t10), B (t40), C (t50), D (t50) and E (t60). The maximum coated sample was the least phosphate concentration remained in the coating solution such as A (t50), B (t20), C (t20), D (t10) and E (t10).

Leaching experiment on the coated pyrite samples was performed according to the procedure described in chapter 3 section 3.2.3.

The results of the leaching experiment measured in terms of pH value and iron concentration in the solution subsequently left after being used for oxidation purpose are shown in Tables 4.5 and 4.6 respectively.

Evidently, the pH values in Table 4.5 measured from the leachate solutions of different reprise of oxidation are ranging from 5.93 to 7.35 which could presumably be considered to be near neutral condition when compared to the acid condition pH 2.78 – 3.88, of controlled sample, of uncoated pyrite. However, the pH in each solution shows tendency to be lower or become more acid when times of repeated oxidation is higher as shown in Figures 4.9 a, 4.10 a, 4.11 a, 4.12 a, and 4.13 a. In contrast, pH of the solution of the uncoated pyrite shows tendency to increase as the number of reaction is higher.

Generally, the iron concentration dissolved in the leachate of the leaching test appears to be highest in the initial batch and then decrease in its content in the subsequent tests (Figures 4.9 b, 4.10 b, 4.11 b, 4.12 b, and 4.13 b). While in the leachate solution of control sample, the iron content decreases abruptly from the initial batch to the next and then decreases gradually thereafter (Figure 4.8). It could be roughly estimated that the amount of iron released from the uncoated pyrite into the solution in the leaching test is at least sixty folds higher than those released from the  $\text{FePO}_4$  coated pyrite samples. This would probably imply that ability of acid mine drainage (AMD) generated from natural pyrite may at least sixty times stronger than the one generated from the coated pyrite.

**Table 4.5** pH in leachates of selected samples after leaching with 0.145 M of hydrogen peroxide solution ( $H_2O_2$ ) at different times.

Time (min.)	pH										
	Solution A		Solution B		Solution C		Solution D		Solution E		Control
	t10	t50	t20	t40	t20	t50	t10	t50	t10	t60	
5	6.90	7.15	7.09	7.10	6.75	6.93	7.25	7.26	7.32	7.30	2.78
60	7.15	7.26	7.23	7.19	6.86	6.86	7.32	7.35	7.30	7.35	2.97
120	6.80	7.07	7.05	6.97	6.65	6.70	7.04	7.04	7.24	7.12	3.75
180	6.72	6.82	6.75	6.86	6.59	6.66	6.95	6.85	6.84	6.90	3.87
240	6.48	6.67	6.68	6.61	6.44	6.40	6.79	6.77	6.74	6.80	3.87
300	6.33	6.53	6.58	6.57	6.26	6.10	6.57	6.66	6.71	6.76	3.88
360	6.18	6.40	6.45	6.48	6.12	5.93	6.54	6.49	6.80	6.72	3.85

**Table 4.6** Iron released in leachates of selected samples after leaching with 0.145 M of hydrogen peroxide solution ( $H_2O_2$ ) at different times.

Time (min.)	Iron released (mg/l)										
	Solution A		Solution B		Solution C		Solution D		Solution E		Control
	t10	t50	t20	t40	t20	t50	t10	t50	t10	t60	
5	0.074	0.038	0.151	0.103	0.343	0.420	0.118	0.218	0.247	0.244	46.20
60	0.083	0.071	0.060	0.063	0.256	0.336	0.166	0.120	0.202	0.102	19.70
120	0.031	0.050	0.045	0	0.115	0.225	0.087	0.150	0.109	0.062	14.65
180	0.035	0.037	0.014	0.070	0.053	0.107	0.124	0.076	0.096	0.109	10.20
240	0.122	0.004	0.008	0.045	0.083	0.101	0.118	0.071	0.089	0.080	14.40
300	0.024	0	0.084	0.073	0.094	0.066	0.045	0.141	0.146	0.109	9.30
360	0	0.077	0.048	0.106	0.104	0.062	0.142	0.023	0.074	0.058	8.70

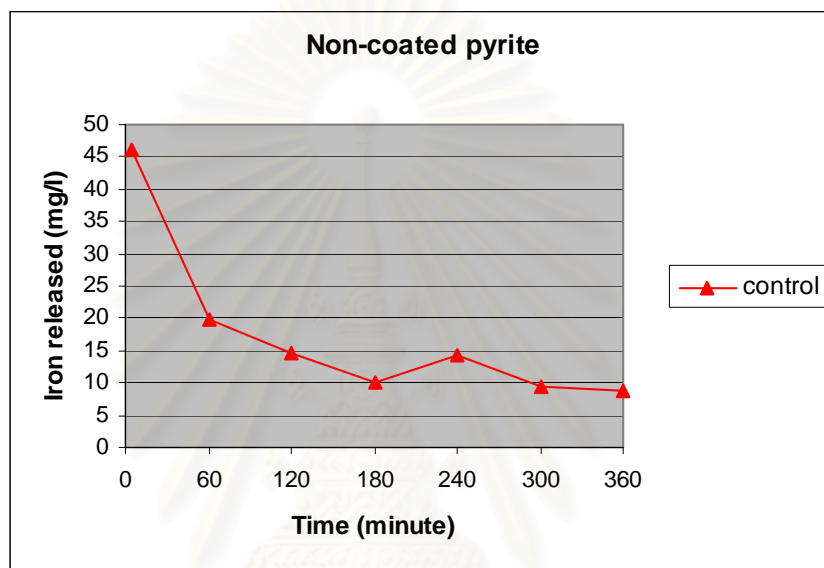
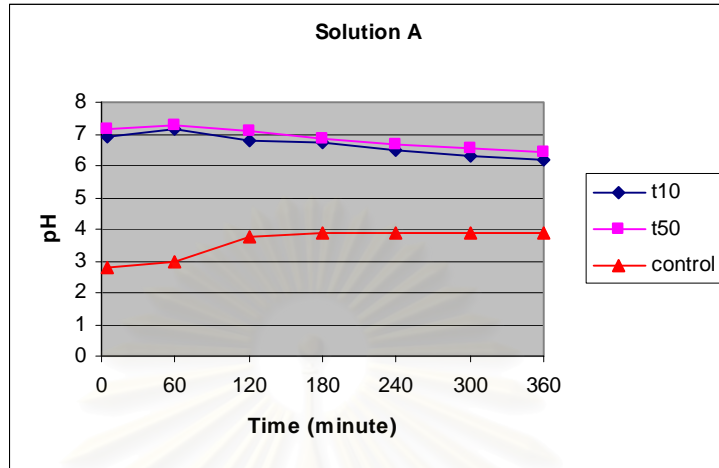
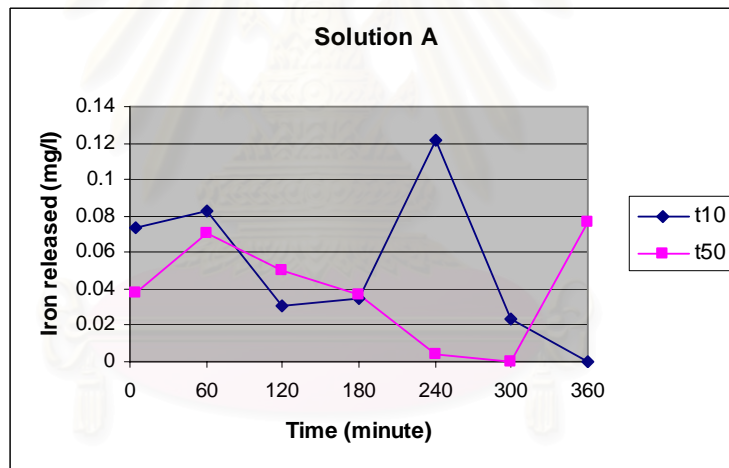


Figure 4.8 Trend of iron released in leachate of uncoted pyrite after leaching with 0.145 M of  $H_2O_2$  solution ( $H_2O_2$ ) at different times.

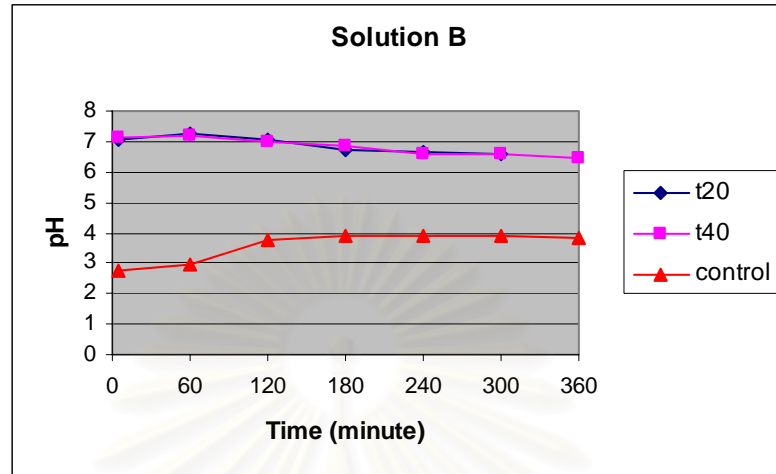


a

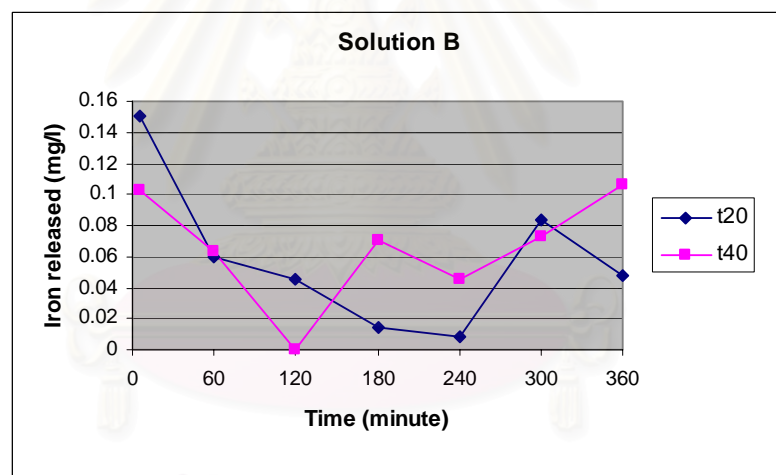


b

Figure 4.9 Trends of pH and iron released in leachates of selected samples solution A after leaching with 0.145 M of  $H_2O_2$  solution ( $H_2O_2$ ) at different times.

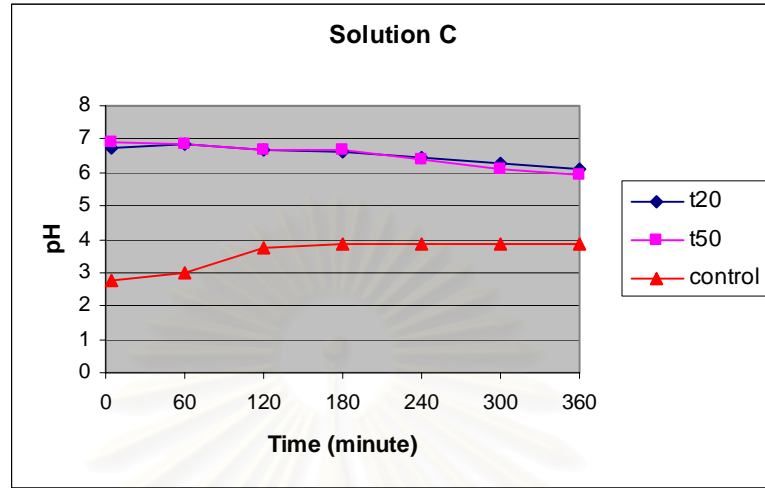


a

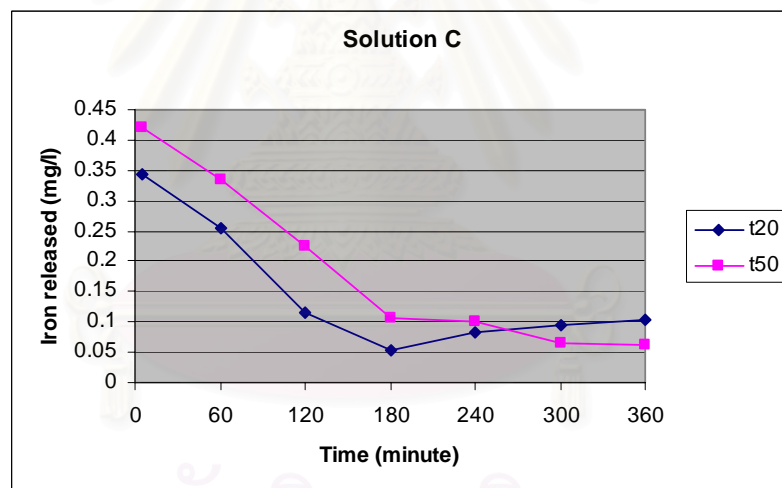


b

Figure 4.10 Trends of pH and iron released in leachates of selected samples solution B after leaching with 0.145 M of  $H_2O_2$  solution ( $H_2O_2$ ) at different times.

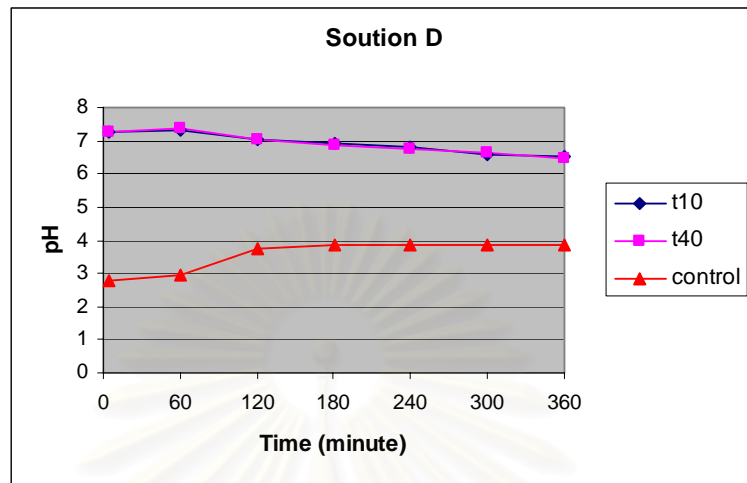


a

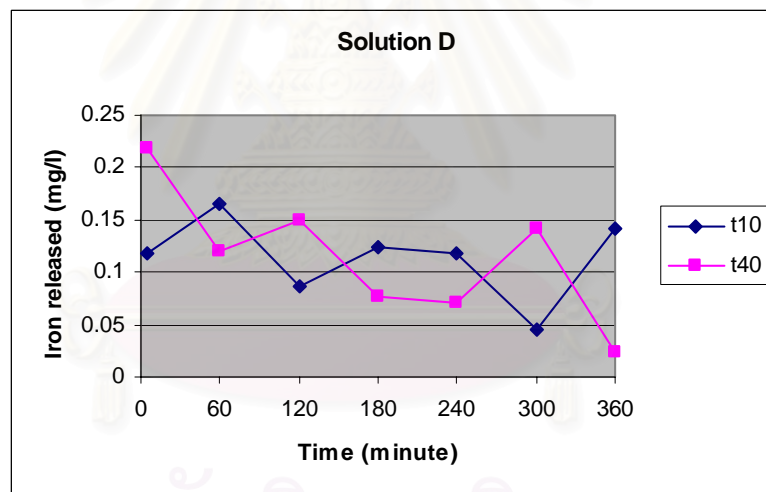


b

Figure 4.11 Trends of pH and iron released in leachates of selected samples solution C after leaching with 0.145 M of  $H_2O_2$  solution ( $H_2O_2$ ) at different times.

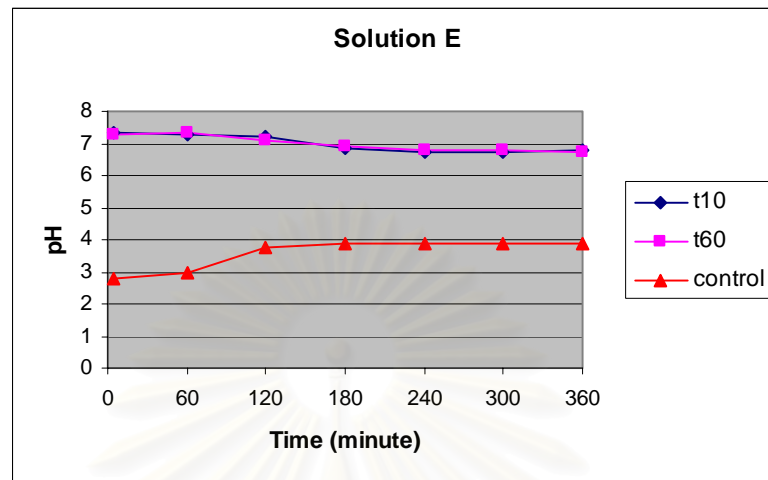


a

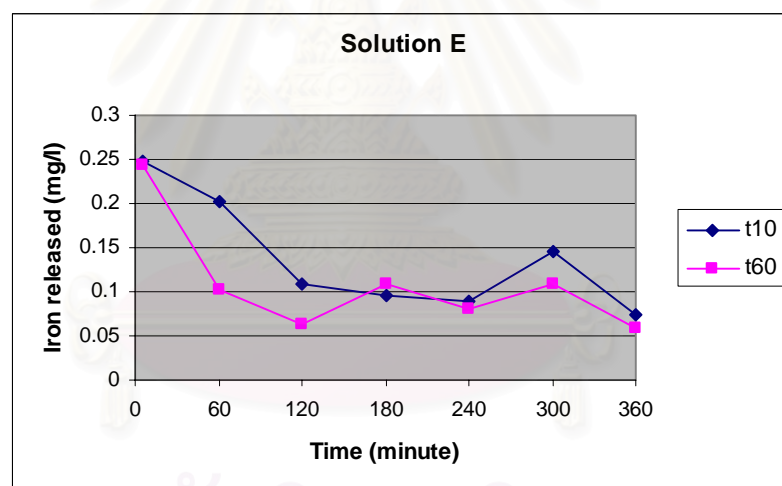


b

Figure 4.12 Trends of pH and iron released in leachates of selected samples solution D after leaching with 0.145 M of  $H_2O_2$  solution ( $H_2O_2$ ) at different times.



a



b

Figure 4.13 Trends of pH and iron released in leachates of selected samples solution E after leaching with 0.145 M of  $H_2O_2$  solution ( $H_2O_2$ ) at different times.

The amount of iron released from leaching test of the coated sample shows prominently decreasing from experiment at t5 to t60, after that iron concentration decreases gradually and stays almost the same throughout t120 and t360. Pyrite oxidation rate would be decrease in accordance to the reduction of iron concentration released in leachates.

The amount of iron released from the coated samples appears to be considerably small. They, however, show also the tendency of decreasing trend. However, their graphic configurations are not as smooth and trendy as that of the control sample. They might show some fluctuations as illustrated in Figures 4.9 b, 4.10 b and 4.12 b.

**Table 4.7** Cumulative iron released in leachates of selected samples after leaching with 0.145 M of hydrogen peroxide solution ( $H_2O_2$ ) at different times.

Time (min.)	Cumulative iron released (mg/l)										
	Solution A		Solution B		Solution C		Solution D		Solution E		Control
	t10	t50	t20	t40	t20	t50	t10	t50	t10	t60	
60	0.157	0.109	0.211	0.166	0.599	0.756	0.284	0.338	0.202	0.346	65.90
120	0.188	0.159	0.256	0.166	0.714	0.981	0.371	0.488	0.311	0.408	80.55
180	0.223	0.196	0.270	0.236	0.767	1.088	0.495	0.564	0.407	0.517	90.75
240	0.345	0.200	0.278	0.281	0.850	1.189	0.613	0.635	0.496	0.597	105.15
300	0.369	0.200	0.362	0.354	0.944	1.255	0.658	0.776	0.642	0.706	114.45
360	0.369	0.277	0.410	0.460	1.048	1.317	0.800	0.799	0.716	0.764	123.15

Table 4.7 and Figure 4.14 show the cumulative amount of iron (Fe) concentration in sequential series of the leaching test. It shows again in this Table and Figure that at least eighty folds of iron content was released from uncoated pyrite in compared to the coated pyrite.

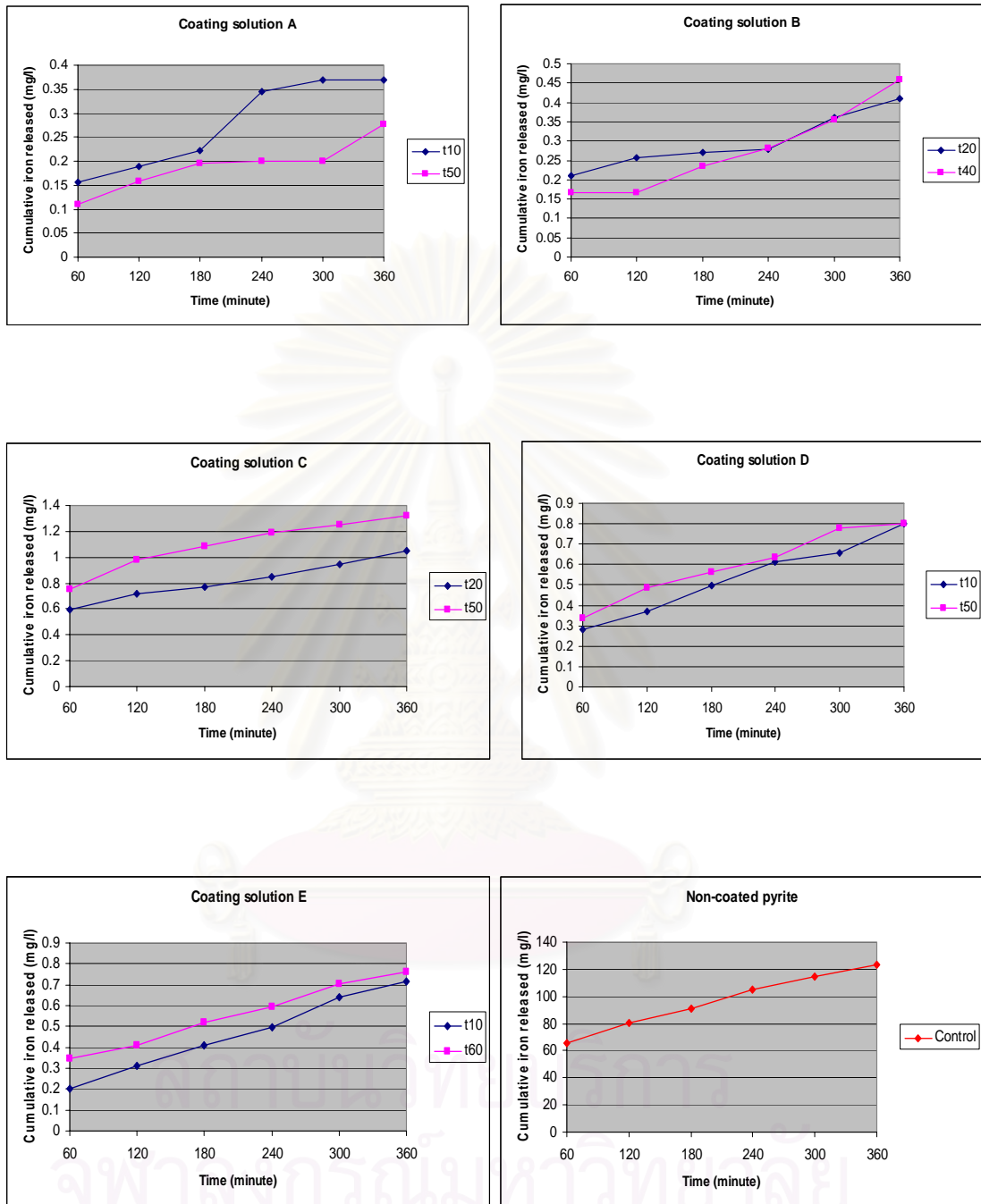
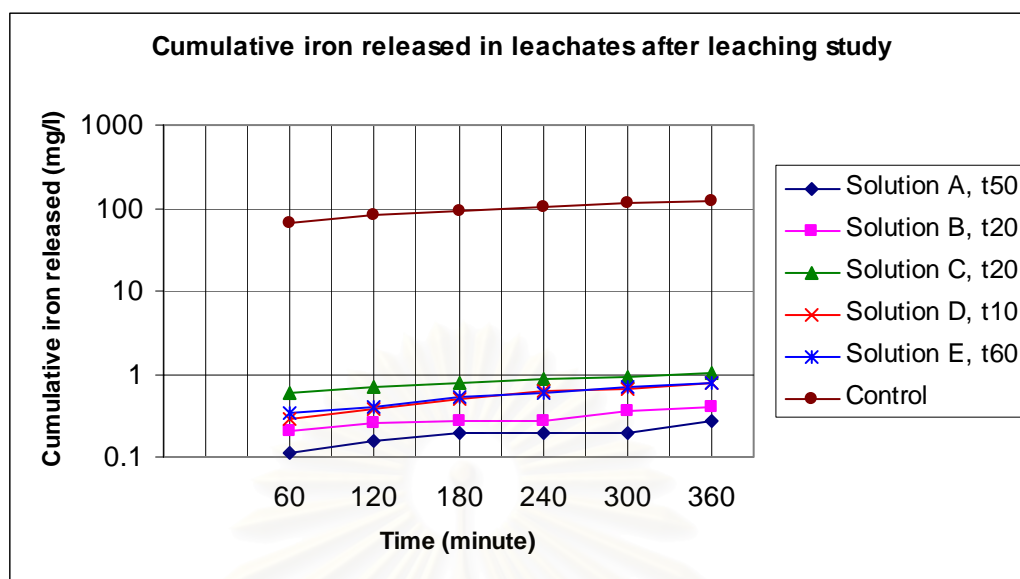


Figure 4.14 The trends of cumulative iron released of selected samples after leaching with 0.145 M of hydrogen peroxide solution ( $H_2O_2$ ) at different times.



**Figure 4.15** The trends of cumulative iron released of samples with the optimum time for coating process after leaching with 0.145 M of hydrogen peroxide solution ( $H_2O_2$ ) at different times.

It could be summarized based on the results of the coating process, the leaching study and the EPMA analysis that the optimum condition of treating pyrite was with the coating solution B ( $0.3 \text{ M } KH_2PO_4 + 0.2 \text{ M } H_2O_2 + 0.2 \text{ M } NaAc$ ) at the optimum time of t20 in the coating process to maximize the formation of an iron-phosphate coating on pyrite surfaces. This was attributed to the quantity of remaining phosphate in solution after coating process was at the lowest concentration (0.497 mg/l). Also, the average content of  $P_2O_5$  on the coated pyrite surface was the highest that is 2.52%. In addition, the concentration of iron released in leachate solution after leaching study was exceptionally low ranging from 0.008 to 0.151 mg/l.

When the pyrite material was treated with the coating solution A ( $0.2 \text{ M } KH_2PO_4 + 0.2 \text{ M } H_2O_2 + 0.2 \text{ M } NaAc$ ) at the optimum time of t50, there was only the results of leaching study that the concentration of iron released in leachate solution after leaching study was quite low ranging from 0.004 to 0.077 mg/l. Because of errors occurred during EPMA analysis, the results including chemical composition on the surface of the

coated pyrite were not available. Owing to the remaining phosphate in solution after coating process was the highest concentration. Thus, it cannot be considered as the optimum condition.

Treating the samples with the coating solution C ( $0.1 \text{ M KH}_2\text{PO}_4 + 0.2 \text{ M H}_2\text{O}_2 + 0.2 \text{ M NaAc}$ ), solution D ( $0.2 \text{ M KH}_2\text{PO}_4 + 0.33 \text{ M H}_2\text{O}_2 + 0.2 \text{ M NaAc}$ ) and solution E ( $0.2 \text{ M KH}_2\text{PO}_4 + 0.01 \text{ M H}_2\text{O}_2 + 0.2 \text{ M NaAc}$ ) in the coating process did not generate the optimum quantity of an iron-phosphate formed on pyrite surfaces. It is also due to the results of remaining phosphate from the coating process did not conform to the results of EPMA analysis. Moreover, the concentrations of iron released in leachates after leaching study were considerably high concentration ranging from 0.045 to 0.343 mg/l.

It could be, therefore, summarized here that, the optimum condition for creating an iron-phosphate coating on pyrite surfaces could be arranged by treating the pyrite with the coating solution B ( $0.3 \text{ M KH}_2\text{PO}_4 + 0.2 \text{ M H}_2\text{O}_2 + 0.2 \text{ M NaAc}$ ) at the optimum time of t20. Iron-phosphate formation on the surfaces of pyrite by treating with this optimum coating solution can efficiently reduce the pyrite oxidation rate and prevent the formation of acid mine drainage (AMD).

#### 4.4 Application for Soil Mining Wastes

The optimum condition of coating iron-phosphate coating material on the pyrite surfaces was obtained experimentally by the process related to the leaching study as described in previous section. Hence, this experimental optimum condition would be used to prove the consistency of the coating material by applying coating solution in the pyrite disseminated soil wastes from a coal mine at Amphoe Lee, Changwat Lumphun (Banpu Public Company Limited). This application is expected to provide the efficiency for coating pyrite in the soil mining wastes. Consequently, they would in turn yield capacity for preventing acid mine drainage (AMD).

Soil mining wastes used in the experiment were collected from three different sampling locations in which they are overburden layer situated on the coal seam. These samples are subsequently labeled as samples A, B and C.

Soil samples A, B and C were treated with the coating solution (0.2 M  $\text{KH}_2\text{PO}_4$  + 0.2 M  $\text{H}_2\text{O}_2$  + 0.2 M NaAc) in columns for creating the coating material. Remaining coating solutions of these samples were analyzed for the pH value.

**Table 4.8** pH of leachates after treating with 200 ml of the coating solution (0.2 M  $\text{KH}_2\text{PO}_4$  + 0.2 M  $\text{H}_2\text{O}_2$  + 0.2 M NaAc) in columns 50 x 500 mm.

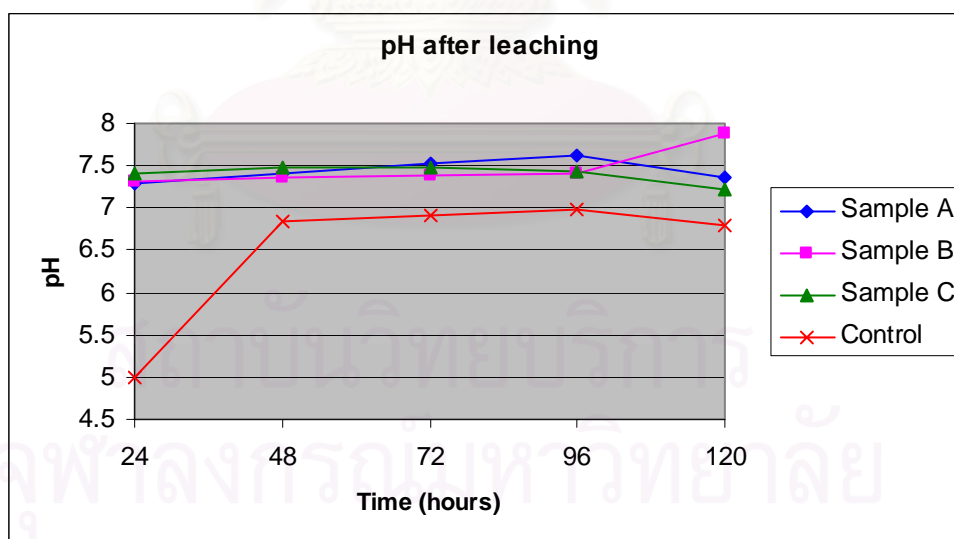
Soil sample	pH
Sample A	5.85
Sample B	5.83
Sample C	5.83

Table 4.8 shows the pH values yielded from remaining coating solution of soil mining wastes after coating process. They vary within narrow range of 5.83 to 5.85.

Subsequently, leaching test of all samples were taken place along with the uncoated control sample that is mixture between sample A, B and C.

**Table 4.9** pH of leachates after leaching with 100 ml oxidizing solution (0.2 M  $\text{H}_2\text{O}_2$ ) at different times (every 24 hours) in columns 50 x 500 mm.

Time (hours)	pH of soil mining wastes			
	Sample A	Sample B	Sample C	Control
24	7.30	7.32	7.42	4.99
48	7.42	7.35	7.49	6.85
72	7.53	7.38	7.49	6.92
96	7.61	7.42	7.43	6.98
120	7.37	7.89	7.23	6.79



**Figure 4.16** Trend of pH after leaching with 100 ml oxidizing solution (0.2 M  $\text{H}_2\text{O}_2$ ) at different times (every 24 hours) in columns 50 x 500 mm.

These samples were leached with the oxidizing solution (0.2 M H<sub>2</sub>O<sub>2</sub>) in the columns for determining the resistance to oxidizing condition. Leachates were measured for pH and analyzed for iron released.

**Table 4.10** Iron released after leaching with 100 ml oxidizing solution (0.2 M H<sub>2</sub>O<sub>2</sub>) at different times (every 24 hours) in columns 50 x 500 mm.

Time (hours)	Iron released (mg/l)			
	Sample A	Sample B	Sample C	Control
24	0.343	0.841	0.356	3.200
48	0.411	0.644	0.313	0.044
72	0.438	1.350	0.408	0
96	0.258	1.020	0.471	0.018
120	0.260	0.305	0.613	0.054

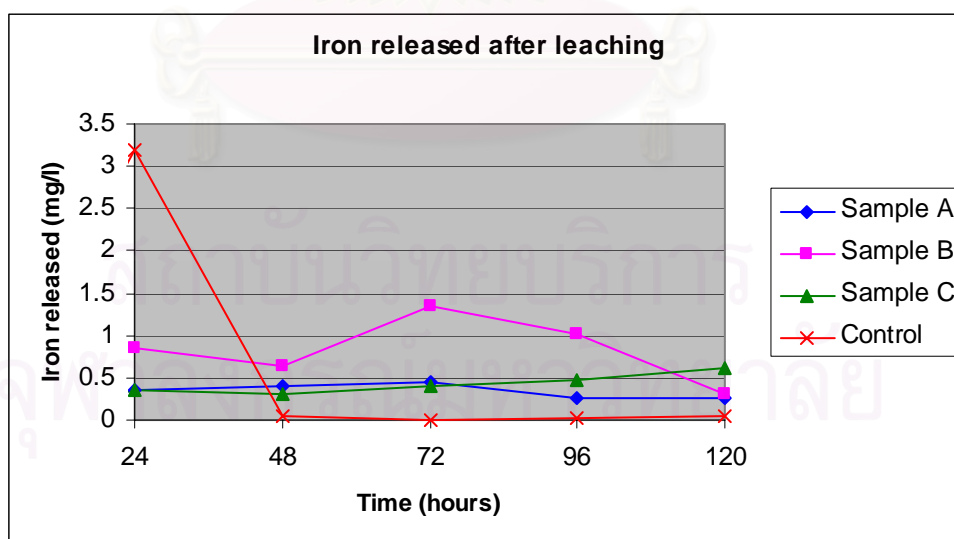


**Figure 4.17** Iron concentrations after leaching with 100 ml oxidizing solution (0.2 M H<sub>2</sub>O<sub>2</sub>) at different times (every 24 hours) in columns 50 x 500 mm.

**Table 4.11** Cumulative iron released from soil mining wastes after leaching with the oxidizing solution at different times.

Time (hours)	Cumulative iron released (mg/l)			
	Sample A	Sample B	Sample C	Control
24	0.343	0.841	0.356	3.200
48	0.754	1.485	0.669	3.244
72	1.192	2.835	1.077	3.244
96	1.450	3.855	1.548	3.262
120	1.710	4.160	2.161	3.316

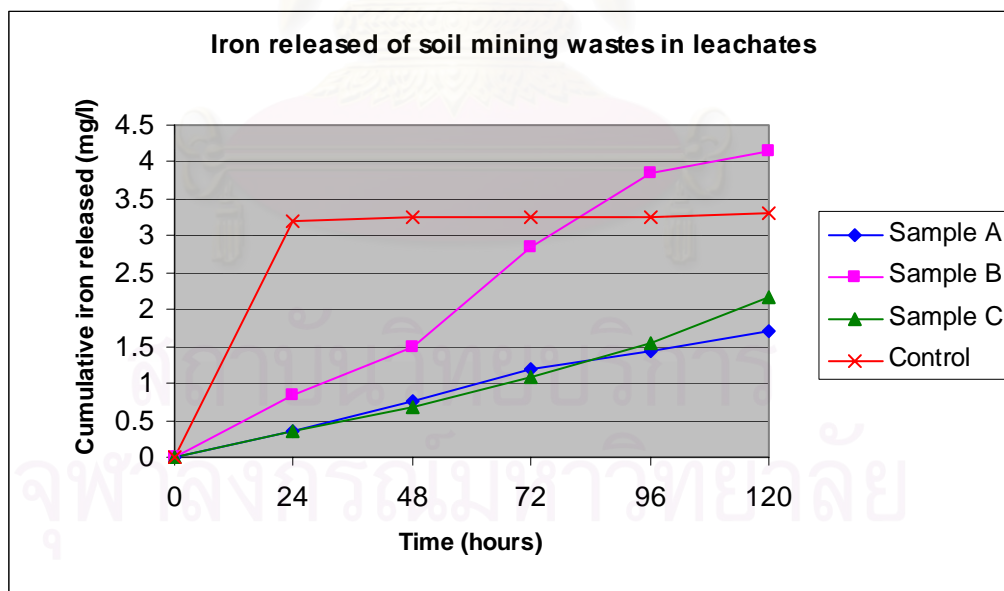


**Figure 4.18** Cumulative iron released from soil mining wastes after leaching with the oxidizing solution at different times.

Table 4.9 and Figure 4.16 reveal pH value of soil mining wastes after leaching with oxidizing solution (0.2 M H<sub>2</sub>O<sub>2</sub>) at different contact times (every 24 hours) that are quite consistent ranging from 7.23 to 7.89. These pH values are higher than the control sample and provided mild base condition. Regarding the trend of pH in leachates, they increase slightly during t<sub>24</sub> and t<sub>72</sub>, and then the pH tendency appears to be decrease afterward. On the other hand, control sample reveal that pH tendency of soil mining wastes is similar to those of pyrite samples. They increase rapidly during t<sub>24</sub> and t<sub>48</sub>, and then the pH is likely stable from t<sub>72</sub> to t<sub>96</sub>.

According to Table 4.10 and Figure 4.17, iron concentrations in leachates are similar to iron contents released from pyrite samples after leaching with oxidizing solution (0.2 M H<sub>2</sub>O<sub>2</sub>) at different times (every 24 hours). Except soil sample B, iron contents released at each contact time in all samples are really high ranging from 0.644 to 1.35 mg/l. In addition, they increase slightly in soil sample C whereas sample A increases slightly from t<sub>24</sub> to t<sub>72</sub>, before it appears to be decreased slightly at t<sub>96</sub> to t<sub>120</sub>. On the other hand, iron contents released from soil sample B are fluctuated in which it has highest concentration at t<sub>72</sub>. Concerning the control sample, trend of iron concentration is similar to pyrite samples. They decrease immediately during t<sub>24</sub> and t<sub>48</sub> and then it appears to be stable.

After application of the selected condition for pyrite coating and leaching test for the soil mining wastes, the iron concentrations released from soil mining wastes are actually higher than the iron contained in leachates of the coated pyrite samples. This result may be caused by the complex composition in soil mining wastes that would contain other minerals such as clay mineral, chalcopyrite (CuFeS<sub>2</sub>), galena (PbS) and sphalerite (ZnS) (Klein and Hurlbut, 1999).

## CHAPTER V

### CONCLUSIONS AND RECOMENDATIONS FOR THE FURTHER STUDIES

#### 5.1 Conclusions

Based on the results of experimental procedures in pyrite samples which include coating process on pyrite surfaces, EPMA (Electron Probe Micro Analyzer) analysis, leaching study and the coating and leaching application in the soil mining wastes, it can be concluded as the following:

In the batch experiment, crushed pyrite samples ( $\text{FeS}_2$ ), and sand of the ratio 1:4 were drenched with coating solution of variant mixture to form the coating substance ( $\text{FeSO}_4$ ), on the surface of pyrite mineral. The reaction between experimental sample (pyrite and sand) was so complete and rapid that only small amount of phosphate was left behind in the spent coating solution in every cases of the experiment, especially when compare this amount with its original concentration in each coating solution. It was believed that high hydraulic conductivity in the batch samples accelerated the reaction rate and considerable amount of coating reaction took place at the surface of iron veiled sand grain. Changing in concentration of  $\text{KH}_2\text{PO}_4$  and  $\text{H}_2\text{O}_2$  in coating solution was designed to determine the optimum combination of these reagents on the formation of the coating material on pyrite surfaces. Apparently, data obtained from the experiment showed that the optimum condition for generation of coating substance was when the samples have been treated.

The pyrite samples coated with the selected coating substance were examined by EPMA (Electron Probe Micro Analyzer) for their chemical compositions of iron-phosphate ( $\text{FePO}_4$ ). The quantity of phosphate on the pyrite surface was high (2.52% of  $\text{P}_2\text{O}_5$ ) after treating with coating solution B reflecting low concentration of phosphate remained in the spent coating solution.

In leaching study, the pyrite samples coated with the different coating solutions was subject to leach with the oxidizing solution of 0.145 M hydrogen peroxide solution ( $H_2O_2$ ) at different contract times. This approach was meant to examine the resistance of the coated pyrite to oxidizing condition after coating process. It was discovered that pyrite when treated with the coating solution A (0.2 M  $KH_2PO_4$  + 0.2 M  $H_2O_2$  + 0.2 M NaAc) at the time of t50 was the optimum condition for creating an iron-phosphate coating on pyrite surfaces. Because pH value was nearly neutral condition (6.40 - 7.26) and there was the lowest concentration of iron released in to the leachate at the amount ranging from 0.004 to 0.077 mg/l.

With the application of the optimum coating solution to the soil mining wastes from coal mine in Amphoe Lee, Changwat Lumphun (Banpu Public Company Limited) reveal that the coating of  $FeSO_4$  on disseminated pyrite in soil was adequate and persistent. This could be deduced from the pH value which ranged from 7.23 to 7.89 and from low concentration of iron released in to the leachates (0.258 - 1.350 mg/l) in the leaching test.

## 5.2 Recommendations for the Further Studies

In this research, there were some limitations for laboratory experiments. Accordingly, it should be required to the advices for the experiments. The suggestions may be useful for the further studies or the relevant works that are the following:

1. The grain size of pyrite samples used in this study should be varied for determining the effect of pyrite surfaces on creating iron-phosphate coating and leaching test with the oxidizing solution.

2. Concerning the leaching study, the ratios of pyrite and sand should be also varied in the loading step. This ratios change may affect the hydraulic conductivity of the mixture sample in column and may have an influence on the oxidation rate of pyrite during leaching with hydrogen peroxide solution ( $H_2O_2$ ) as the oxidizing solution.

3. The experimental feeding of oxidizing solution ( $H_2O_2$ ) during leaching test in columns should be fed continuously for determining the flow rate through the columns and perfectly evaluating the effectiveness of the coated pyrite resisted to the oxidizing condition.

4. The concentration of hydrogen peroxide ( $H_2O_2$ ) should be really varied for examining the iron released as well as the pyrite oxidation rate during leaching study. Moreover, it should be compared between leaching with distilled water and leaching with various concentrations of the oxidizing solution.

5. About analysis, sulfate concentration should be analyzed for estimating the degree of oxidation during coating process. Sulfate can be a good index of pyrite oxidation only during the coating process because free sulfur is not formed under this condition (Georgopoulou et al., 1995).

6. As regards the application with soil mining wastes, coating step that is treating with coating solution was only conducted in the coating process, conversely, stabilizing with  $Ca(OH)_2$  solution was not performed during this coating process. It results in quite low quality of coating substances. Thus, it must be stabilized during coating process in order to firmly stabilize the existence of these coating substances.

## REFERENCES

- Adams, R.L., Ninestee, J.J., and Rauch, H.W. 1994. Laboratory testing of coatings for prevention of acid drainage in underground coal mines. Proceedings of second international conference on the abatement of acid drainage, Pittsburgh, PA, 24-29 April, United States Bureau of Mines Special Publication SP O6A-94. 2: 321.
- Eaton, A.D., Clesceri, L.S., and Greenberg A.E. 1995. Standard methods for the examination of water and wastewater. 19<sup>th</sup> edition. Washington, DC: American Public Health Association.
- Evangelou, V.P. 2001. Pyrite microencapsulation technologies: Principles and potential field application. Ecological Engineering 17: 165-178.
- Evangelou, V.P., and Huang, X. 1992. A new technology for armoring and deactivating pyrite. In: Singhal and others (Ed). Environmental issues and waste management in energy and minerals Production. Amsterdam Netherlands : AA Balkema: 413-417.
- Garcin, M. 2003. Factors affecting AMD generation[Online]. Available from: [www.brgm.fr/mineo/UserNeed/IMPACTS.pdf](http://www.brgm.fr/mineo/UserNeed/IMPACTS.pdf)
- Georgopoulou, Z.J., Fytas, K., Soto, H., and Evangelou, B. 1995. Feasibility and cost of creating an iron-phosphate coating on pyrrhotite to prevent oxidation. Environmental Geology 28: 61-69.
- Klein, C., and Hurlbut, C.S. 1999. Manual of mineralogy. 21<sup>st</sup> edition, revised. Canada: John Wiley & Sons.

- Kleinmann, R.L.P., Crerar, D.A., and Pacelli, R.R. 1981. Biogeochemistry of acid mine drainage and a method to control acid formation. Mining Engineering 33: 300-303.
- Monterroso, C., and Macias, F. 1998. Drainage waters affected by pyrite oxidation in a coal mine in Galicia (NW Spain): composition and mineral stability. Sci. Total Environ 216: 121-132.
- Nyavor, K., and Egiebor, N.O. 1995. Control of pyrite oxidation by phosphate coating. The Science of the Total Environment 162: 225-237.
- Rose, A.W., and Cravotta, C.A. 1994. Geochemistry of coal mine drainage[Online]. Available from: [www.dep.state.pa.us/dep/deputate/minres/districts/cmdp/chap01.html](http://www.dep.state.pa.us/dep/deputate/minres/districts/cmdp/chap01.html)
- Seif, J.M. 1994. The science of acid mine drainage and passive treatment[Online]. Available from: [www.dep.state.pa.us/dep/deputate/minres/bamr/amd/science\\_of\\_amd.html](http://www.dep.state.pa.us/dep/deputate/minres/bamr/amd/science_of_amd.html)
- Singer, P.C., and Stumm, W. 1970. Acid mine drainage: Rate determining step. Science 167: 1121-1123.
- Vandiviere, M.M., and Evangelou, V.P. 1998. Comparative testing between conventional and microencapsulation approaches in controlling pyrite oxidation. Journal of Geochemical Exploration 64: 161-176.
- Wittke, J.H. 1997. Electron Interaction with Matter[Online]. Available from: [www.cameca.fr/html/epma\\_technique.html](http://www.cameca.fr/html/epma_technique.html)[2005, April 5]
- Zhang, Y.L., and Evangelou, V.P. 1998. Formation of ferric hydroxide-silica coatings on pyrite and its oxidation behavior. Soil Science 163: 53-62.



APPENDIX

สถาบันวิทยบริการ  
จุฬาลงกรณ์มหาวิทยาลัย

Sample Mass proportion (%)													
	nc1-1	nc1-2	nc1-3	nc1-4	nc2-1	nc2-2	nc2-3	nc2-4	nc2-5	nc3-1	nc3-2	nc3-3	nc3-4
K <sub>2</sub> O	0.01	0.00	0.00	0.01	0.00	0.02	0.00	0.01	0.01	0.00	0.00	0.01	0.10
CaO	0.00	0.01	0.04	0.01	0.02	0.01	0.00	0.01	0.01	0.00	0.01	0.02	0.08
FeO	63.77	62.18	62.97	63.12	63.54	63.20	62.49	64.04	64.04	56.34	53.05	52.23	
Na <sub>2</sub> O	0.01	0.03	0.02	0.01	0.03	0.03	0.02	0.01	0.00	0.07	0.08	0.01	0.02
BaO	0.00	0.04	0.06	0.00	0.00	0.02	0.00	0.00	0.00	0.00	0.00	0.00	0.02
MnO	0.01	0.00	0.04	0.00	0.00	0.00	0.00	0.00	0.00	0.02	0.00	0.00	0.04
MgO	0.00	0.01	0.00	0.02	0.00	0.00	0.00	0.00	0.07	0.09	0.03	0.24	0.40
SiO <sub>2</sub>	0.04	0.09	0.11	0.05	0.09	0.07	0.10	0.06	0.07	0.07	0.05	0.16	1.77
SO <sub>3</sub>	137.59	136.29	133.99	136.23	137.57	136.83	137.01	138.52	138.20	138.35	126.29	136.65	
Al <sub>2</sub> O <sub>3</sub>	0.00	0.05	0.06	0.02	0.04	0.03	0.03	0.02	0.00	0.11	0.07	0.12	0.43
P <sub>2</sub> O <sub>5</sub>	0.03	0.00	0.02	0.00	0.00	0.00	0.00	0.00	0.03	0.03	0.01	0.00	0.04
Total	201.46	198.69	197.31	199.46	201.28	200.22	199.64	202.65	202.43	195.08	179.59	189.44	129.77

<b>Sample</b> <b>Mass proportion (%)</b>	nc4-1	nc4-2	nc4-3	nc4-4	nc4-5	b1-1	b1-2	b1-3	b1-4	b2-1	b2-2	b2-3	b2-4
K <sub>2</sub> O	0.03	0.05	0.02	0.01	0.01	0.26	0.36	0.37	0.21	0.80	0.88	1.07	0.70
CaO	0.01	0.02	0.00	0.01	0.01	0.31	2.11	2.04	0.52	0.53	1.01	3.19	0.87
FeO	64.01	63.49	64.06	64.52	64.06	63.55	54.05	58.81	63.81	63.83		45.22	60.01
Na <sub>2</sub> O	0.02	0.00	0.03	0.04	0.04	0.36	0.33	0.47	0.20	0.71	0.91	1.39	0.86
BaO	0.00	0.01	0.05	0.00	0.03	0.07	0.00	0.02	0.01	0.00	0.00	0.00	0.05
MnO	0.00	0.01	0.03	0.00	0.04	0.05	0.00	0.02	0.01	0.03	0.01	0.07	0.00
MgO	0.11	0.00	0.00	0.00	0.02	0.04	0.20	0.16	0.05	0.22	6.53	0.58	0.23
SiO <sub>2</sub>	0.25	0.09	0.01	0.00	0.09	0.10	0.25	0.17	0.08	0.09	11.00	0.66	0.30
SO <sub>3</sub>	138.12	137.59	138.84	139.83	137.30	134.66	121.98	128.59	134.33	132.11		105.00	128.00
Al <sub>2</sub> O <sub>3</sub>	0.01	0.03	0.02	0.00	0.04	0.07	0.12	0.17	0.05	0.03	0.20	0.28	0.20
P <sub>2</sub> O <sub>5</sub>	0.02	0.00	0.01	0.01	0.01	1.05	2.78	2.56	1.18	1.83	2.48	6.30	2.72
Total	202.56	201.30	203.07	204.41	201.63	200.53	182.17	193.38	200.44	200.18	158.42	163.76	193.92

<b>Sample</b> <b>Mass proportion (%)</b>	b3-1	b3-2	b3-3	b3-4	b4-1	b4-2	b4-3	b4-4	b5-1	b5-2	b5-3	b5-4	b6-1
K <sub>2</sub> O	0.57	1.40	1.50	0.29	0.43	0.30	0.19	0.73	0.45	0.41	0.35	0.39	0.65
CaO	0.64	4.12	5.67	0.50	0.24	0.71	0.30	0.42	0.21	0.13	0.19	0.38	1.55
FeO	62.78			58.85		56.76	52.12	50.56	65.06	64.89	63.39	63.39	59.18
Na <sub>2</sub> O	0.59	0.72	0.73	0.32	0.19	0.24	0.15	0.51	0.50	0.45	0.45	0.55	0.60
BaO	0.00	0.00	0.02	0.00	0.00	0.04	0.00	0.05	0.06	0.00	0.06	0.00	0.00
MnO	0.03	0.08	0.10	0.01	0.00	0.06	0.00	0.01	0.01	0.00	0.00	0.05	0.00
MgO	0.10	0.16	0.46	0.08	0.21	0.18	0.08	0.16	0.09	0.09	0.13	0.08	0.28
SiO <sub>2</sub>	0.12	0.78	1.94	0.31	0.41	0.34	0.07	0.75	0.11	0.08	0.13	0.23	0.28
SO <sub>3</sub>	129.76			127.99		124.32	119.60	114.82	135.72	139.57	135.06	135.78	125.69
Al <sub>2</sub> O <sub>3</sub>	0.09	0.48	1.14	0.26	0.10	0.09	0.05	0.23	0.09	0.06	0.08	0.16	0.07
P <sub>2</sub> O <sub>5</sub>	2.11	5.29	11.11	1.43	1.24	1.29	1.05	2.51	1.16	1.04	1.04	1.37	2.83
Total	196.79	105.41	114.77	190.04	65.31	184.33	173.61	170.74	203.45	206.72	200.87	202.37	191.12

<b>Sample</b> <b>Mass proportion (%)</b>	b6-2	b6-3	b6-4	c1-1	c1-2	c1-3	c1-4	c2-1	c2-2	c2-3	c2-4	c3-1	c3-2
K <sub>2</sub> O	0.21	0.38	0.43	0.09	0.19	0.14	1.10	0.54	0.19	0.11	0.18	0.21	0.33
CaO	0.91	1.50	0.49	0.11	0.14	0.11	0.69	3.68	1.23	0.50	0.61	0.36	0.47
FeO	60.37	60.07	51.42	63.40	63.64	62.11	57.34	50.09	60.53	62.00	58.03	62.64	60.32
Na <sub>2</sub> O	0.38	0.75	0.34	0.19	0.43	0.42	1.00	1.81	0.96	0.46	0.69	1.05	1.38
BaO	0.00	0.00	0.00	0.00	0.00	0.00	0.04	0.00	0.03	0.00	0.01	0.00	0.03
MnO	0.00	0.02	0.01	0.00	0.04	0.00	0.00	0.00	0.00	0.01	0.00	0.03	0.00
MgO	0.38	0.23	0.04	0.03	0.07	0.04	0.31	0.19	0.09	0.07	0.12	0.12	0.17
SiO <sub>2</sub>	0.52	0.10	0.08	0.06	0.04	0.14	0.85	0.20	0.09	0.16	0.35	0.09	0.40
SO <sub>3</sub>	127.94	129.44	119.39	136.41	135.54	133.01	126.32	107.54	129.93	132.10	125.94	131.94	127.69
Al <sub>2</sub> O <sub>3</sub>	0.15	0.07	0.05	0.03	0.04	0.03	0.37	0.18	0.09	0.05	0.17	0.03	0.09
P <sub>2</sub> O <sub>5</sub>	1.54	3.12	1.59	0.55	1.04	0.93	1.69	4.79	1.90	0.66	1.49	1.33	2.02
Total	192.40	195.68	173.85	200.87	201.17	196.95	189.71	169.02	195.03	196.13	187.58	197.79	192.91

<b>Sample</b> <b>Mass proportion (%)</b>	c3-3	c3-4	c4-1	c4-2	c4-3	c4-4	c5-1	c5-2	c5-3	c5-4	c5-5	c6-1	c6-2
K <sub>2</sub> O	0.24	0.36	0.42	0.14	0.39	0.35	0.16	0.11	0.15	0.20	0.08	0.09	0.24
CaO	0.33	1.00	1.39	0.32	1.75	1.15	0.84	0.36	0.81	0.55	0.29	0.11	0.69
FeO	61.93	59.81	57.47	61.75	54.90	58.15	62.28	62.64	61.22	61.60	63.58	63.39	58.49
Na <sub>2</sub> O	0.76	1.39	1.84	0.72	1.99	1.39	0.72	0.33	0.55	0.64	0.36	0.38	0.88
BaO	0.00	0.00	0.00	0.00	0.00	0.02	0.00	0.00	0.00	0.05	0.02	0.00	0.01
MnO	0.07	0.04	0.06	0.00	0.00	0.05	0.06	0.00	0.00	0.00	0.00	0.00	0.04
MgO	0.09	0.21	1.05	0.29	1.02	0.75	0.08	0.18	0.40	0.05	0.06	0.02	0.17
SiO <sub>2</sub>	0.09	0.20	0.33	0.11	0.15	0.09	0.09	0.42	0.75	0.06	0.12	0.07	0.24
SO <sub>3</sub>	132.43	128.79	125.59	132.57	119.52	128.57	133.76	136.71	132.32	132.49	136.34	135.39	127.05
Al <sub>2</sub> O <sub>3</sub>	0.05	0.07	0.06	0.03	0.04	0.02	0.05	0.05	0.12	0.03	0.05	0.04	0.07
P <sub>2</sub> O <sub>5</sub>	1.11	2.50	4.41	1.60	4.39	3.66	1.30	0.55	1.12	1.15	0.65	0.50	1.45
Total	197.10	194.38	192.59	197.52	184.15	194.20	199.35	201.36	197.44	196.82	201.54	199.98	189.31

<b>Sample</b> <b>Mass proportion (%)</b>	c6-3	c6-4	c6-5	c6-6	d1-1	d1-2	d1-3	d2-1	d2-2	d2-3	d2-4	d2-5	d3-1
K <sub>2</sub> O	0.30	0.13	0.12	0.04	0.19	0.19	0.24	0.16	1.20	0.09	0.16	0.14	0.81
CaO	0.25	0.27	0.30	0.11	1.04	0.57	1.19	0.32	0.89	0.21	0.33	0.28	1.29
FeO	56.94	61.04	62.33	63.32	53.18	55.77	53.21	61.81	53.15	62.50	60.20	61.77	57.57
Na <sub>2</sub> O	0.87	0.39	0.32	0.21	0.35	0.41	0.40	0.22	1.25	0.20	0.29	0.27	1.63
BaO	0.05	0.00	0.01	0.00	0.00	0.00	0.00	0.00	0.00	0.00	0.00	0.01	0.01
MnO	0.06	0.03	0.01	0.00	0.00	0.04	0.04	0.05	0.05	0.00	0.03	0.00	0.01
MgO	0.11	0.20	0.01	0.03	0.10	0.12	0.20	0.00	0.08	0.02	0.07	0.05	0.22
SiO <sub>2</sub>	2.46	0.31	0.55	0.24	0.10	0.44	0.45	0.04	0.60	0.04	0.19	0.22	0.14
SO <sub>3</sub>	123.97	134.78	134.67	135.59	124.01	127.52	121.90	131.01	104.96	134.82	122.03	132.79	124.32
Al <sub>2</sub> O <sub>3</sub>	0.30	0.05	0.27	0.02	0.02	0.08	0.07	0.05	0.24	0.04	0.10	0.09	0.08
P <sub>2</sub> O <sub>5</sub>	1.10	0.82	0.72	0.41	1.15	1.09	1.90	0.80	4.63	0.64	0.56	0.89	4.06
Total	186.40	198.02	199.31	199.97	180.15	186.24	179.61	194.46	167.04	198.54	183.95	196.50	190.14

<b>Sample</b> <b>Mass proportion (%)</b>	d3-2	d3-3	d3-4	d4-1	d4-2	d4-3	d4-4	d4-5	e1-1	e1-2	e1-3	e1-4	e2-1
K <sub>2</sub> O	0.75	0.16	0.33	0.83	0.45	0.38	0.45	0.35	0.32	0.59	1.78	0.58	0.26
CaO	1.17	0.08	0.54	0.93	0.32	0.36	0.32	0.37	0.26	1.17	8.11	0.81	0.39
FeO	58.18	62.76	60.63	56.71	60.82	60.42	60.72	62.10	64.40	58.64		62.41	62.52
Na <sub>2</sub> O	1.60	0.35	0.82	1.52	0.82	0.67	0.75	0.48	0.76	1.39	3.43	1.54	0.76
BaO	0.04	0.00	0.00	0.00	0.01	0.00	0.00	0.00	0.00	0.04	0.04	0.00	0.00
MnO	0.01	0.00	0.05	0.03	0.04	0.00	0.05	0.07	0.00	0.01	0.03	0.00	0.05
MgO	0.18	0.03	0.12	0.53	0.18	0.15	0.17	0.15	0.08	0.43	1.53	0.22	0.30
SiO <sub>2</sub>	0.04	0.02	0.08	0.61	0.17	0.07	0.08	0.05	0.24	0.24	0.86	0.17	0.34
SO <sub>3</sub>	127.86	136.30	131.10	125.75	131.08	132.83	131.94	134.71	133.92	125.83		129.06	132.27
Al <sub>2</sub> O <sub>3</sub>	0.06	0.02	0.03	0.10	0.05	0.07	0.06	0.05	0.14	0.09	0.44	0.07	0.06
P <sub>2</sub> O <sub>5</sub>	3.62	0.56	2.01	3.51	1.89	1.48	1.70	1.08	1.33	3.54	16.20	2.94	1.23
Total	193.50	200.27	195.71	190.51	195.81	196.43	196.23	199.40	201.44	191.96	147.81	197.79	198.16

<b>Sample</b> <b>Mass proportion (%)</b>	e2-2	e2-3	e2-4	e3-1	e3-2	e3-3	e3-4	e4-1	e4-2	e4-3	e4-4	e4-5	e5-1
K <sub>2</sub> O	0.41	0.47	0.23	0.60	0.17	0.18	0.14	0.70	0.37	0.28	0.25	0.28	0.28
CaO	0.54	1.91	0.71	1.84	0.35	0.20	0.23	0.67	0.55	0.20	0.27	0.35	0.47
FeO	60.72	57.39	63.11	57.75	63.28	65.04	64.32	57.87	61.78	63.94	64.24	62.05	63.30
Na <sub>2</sub> O	1.08	1.32	0.55	1.41	0.44	0.45	0.36	1.84	1.14	0.75	0.63	0.78	0.78
BaO	0.00	0.00	0.00	0.04	0.08	0.06	0.00	0.06	0.00	0.04	0.00	0.09	0.05
MnO	0.01	0.00	0.00	0.02	0.00	0.01	0.03	0.02	0.00	0.02	0.01	0.02	0.00
MgO	0.20	0.33	0.15	0.49	0.13	0.11	0.15	0.45	0.26	0.17	0.23	0.25	0.16
SiO <sub>2</sub>	0.55	0.10	0.17	0.12	0.09	0.04	0.10	0.28	0.17	0.05	0.17	0.04	0.11
SO <sub>3</sub>	129.43	123.39	133.41	124.01	135.56	137.44	139.51	125.77	131.67	134.99	135.78	133.46	134.30
Al <sub>2</sub> O <sub>3</sub>	0.28	0.09	0.07	0.11	0.05	0.04	0.04	0.09	0.04	0.02	0.08	0.01	0.06
P <sub>2</sub> O <sub>5</sub>	1.62	2.59	1.04	4.63	1.12	0.88	0.84	3.12	1.87	1.32	1.11	1.48	1.61
Total	194.83	187.60	199.43	191.03	201.26	204.43	205.72	190.86	197.85	201.77	202.77	198.81	201.14

Sample Mass proportion (%)	Sample			
	e5-2	e5-3	e5-4	e5-5
K <sub>2</sub> O	0.20	0.12	1.67	0.18
CaO	0.34	0.10	0.74	0.20
FeO	62.75	65.64	37.89	64.08
Na <sub>2</sub> O	0.61	0.39	1.29	0.47
BaO	0.07	0.00	0.00	0.05
MnO	0.00	0.01	0.01	0.00
MgO	0.22	0.09	0.52	0.11
SiO <sub>2</sub>	0.24	0.02	0.80	0.03
SO <sub>3</sub>	135.80	138.93	109.64	136.77
Al <sub>2</sub> O <sub>3</sub>	0.08	0.00	0.30	0.01
P <sub>2</sub> O <sub>5</sub>	1.40	0.69	3.60	0.98
Total	201.71	205.97	156.45	202.88

จุฬาลงกรณ์มหาวิทยาลัย

Sample Atomic proportion	nc1-1	nc1-2	nc1-3	nc1-4	nc2-1	nc2-2	nc2-3	nc2-4	nc2-5	nc3-1	nc3-2	nc3-3	nc3-4
K	0.000	0.000	0.000	0.000	0.000	0.000	0.000	0.000	0.000	0.000	0.000	0.000	0.027
Ca	0.000	0.000	0.000	0.000	0.000	0.000	0.000	0.000	0.000	0.000	0.000	0.000	0.017
Fe	0.147	0.145	0.148	0.147	0.146	0.146	0.145	0.147	0.147	0.131	0.135	0.124	0.000
Na	0.000	0.000	0.000	0.000	0.000	0.000	0.000	0.000	0.000	0.000	0.000	0.000	0.008
Ba	0.000	0.000	0.000	0.000	0.000	0.000	0.000	0.000	0.000	0.000	0.000	0.000	0.002
Mn	0.000	0.000	0.000	0.000	0.000	0.000	0.000	0.000	0.000	0.000	0.000	0.000	0.007
Mg	0.000	0.000	0.000	0.000	0.000	0.000	0.000	0.000	0.000	0.000	0.000	0.001	0.126
Si	0.000	0.000	0.000	0.000	0.000	0.000	0.000	0.000	0.000	0.000	0.000	0.000	0.376
S	0.284	0.285	0.283	0.284	0.284	0.284	0.285	0.284	0.284	0.289	0.288	0.291	0.000
Al	0.000	0.000	0.000	0.000	0.000	0.000	0.000	0.000	0.000	0.000	0.000	0.000	0.107
P	0.000	0.000	0.000	0.000	0.000	0.000	0.000	0.000	0.000	0.000	0.000	0.000	0.006
Fe : S	0.516	0.508	0.524	0.516	0.515	0.515	0.508	0.515	0.516	0.454	0.468	0.426	
S : P													

Sample Atomic proportion	nc4-1	nc4-2	nc4-3	nc4-4	nc4-5	b1-1	b1-2	b1-3	b1-4	b2-1	b2-2	b2-3	b2-4
K	0.000	0.000	0.000	0.000	0.000	0.001	0.001	0.001	0.001	0.003	0.031	0.005	0.003
Ca	0.000	0.000	0.000	0.000	0.000	0.001	0.007	0.006	0.002	0.002	0.030	0.012	0.003
Fe	0.147	0.146	0.146	0.146	0.148	0.148	0.139	0.143	0.149	0.151	0.000	0.131	0.146
Na	0.000	0.000	0.000	0.000	0.000	0.002	0.002	0.003	0.001	0.004	0.048	0.009	0.005
Ba	0.000	0.000	0.000	0.000	0.000	0.000	0.000	0.000	0.000	0.000	0.000	0.000	0.000
Mn	0.000	0.000	0.000	0.000	0.000	0.000	0.000	0.000	0.000	0.000	0.000	0.000	0.000
Mg	0.000	0.000	0.000	0.000	0.000	0.000	0.001	0.001	0.000	0.001	0.268	0.003	0.001
Si	0.001	0.000	0.000	0.000	0.000	0.000	0.001	0.000	0.000	0.000	0.303	0.002	0.001
S	0.284	0.284	0.284	0.285	0.284	0.282	0.281	0.280	0.282	0.280	0.000	0.274	0.279
Al	0.000	0.000	0.000	0.000	0.000	0.000	0.000	0.001	0.000	0.000	0.006	0.001	0.001
P	0.000	0.000	0.000	0.000	0.000	0.002	0.007	0.006	0.003	0.004	0.058	0.019	0.007
Fe : S	0.516	0.514	0.514	0.514	0.520	0.526	0.494	0.510	0.529	0.538		0.480	0.522
S : P						113.913	38.967	44.512	101.091	64.000	0.000	14.785	41.795

<b>Sample</b>	b3-1	b3-2	b3-3	b3-4	b4-1	b4-2	b4-3	b4-4	b5-1	b5-2	b5-3	b5-4	b6-1
<b>Atomic proportion</b>													
K	0.002	0.136	0.079	0.001	0.180	0.001	0.001	0.003	0.002	0.001	0.001	0.001	0.002
Ca	0.002	0.337	0.250	0.002	0.086	0.002	0.001	0.001	0.001	0.000	0.001	0.001	0.005
Fe	0.151	0.000	0.000	0.144	0.000	0.143	0.138	0.138	0.150	0.146	0.148	0.147	0.146
Na	0.003	0.107	0.058	0.002	0.122	0.001	0.001	0.003	0.003	0.002	0.002	0.003	0.003
Ba	0.000	0.000	0.000	0.000	0.000	0.000	0.000	0.000	0.000	0.000	0.000	0.000	0.000
Mn	0.000	0.005	0.004	0.000	0.001	0.000	0.000	0.000	0.000	0.000	0.000	0.000	0.000
Mg	0.000	0.018	0.028	0.000	0.105	0.001	0.000	0.001	0.000	0.000	0.001	0.000	0.001
Si	0.000	0.060	0.080	0.001	0.135	0.001	0.000	0.002	0.000	0.000	0.000	0.001	0.001
S	0.279	0.000	0.000	0.282	0.000	0.282	0.285	0.281	0.281	0.283	0.282	0.282	0.279
Al	0.000	0.043	0.055	0.001	0.039	0.000	0.000	0.001	0.000	0.000	0.000	0.001	0.000
P	0.005	0.342	0.387	0.004	0.347	0.003	0.003	0.007	0.003	0.002	0.002	0.003	0.007
Fe : S	0.539			0.512	0.509	0.486	0.491	0.534	0.518	0.523	0.520	0.525	
S : P	54.649	0.000	0.000	79.345	0.000	85.433	101.363	40.520	103.718	118.518	114.792	88.116	39.401

<b>Sample</b> <b>Atomic proportion</b>	b6-2	b6-3	b6-4	c1-1	c1-2	c1-3	c1-4	c2-1	c2-2	c2-3	c2-4	c3-1	c3-2
K	0.001	0.001	0.002	0.000	0.001	0.001	0.004	0.002	0.001	0.000	0.001	0.001	0.001
Ca	0.003	0.005	0.002	0.000	0.000	0.000	0.002	0.013	0.004	0.002	0.002	0.001	0.001
Fe	0.147	0.144	0.137	0.147	0.148	0.147	0.142	0.142	0.146	0.148	0.145	0.149	0.147
Na	0.002	0.004	0.002	0.001	0.002	0.002	0.006	0.012	0.005	0.003	0.004	0.006	0.008
Ba	0.000	0.000	0.000	0.000	0.000	0.000	0.000	0.000	0.000	0.000	0.000	0.000	0.000
Mn	0.000	0.000	0.000	0.000	0.000	0.000	0.000	0.000	0.000	0.000	0.000	0.000	0.000
Mg	0.002	0.001	0.000	0.000	0.000	0.000	0.001	0.001	0.000	0.000	0.001	0.000	0.001
Si	0.002	0.000	0.000	0.000	0.000	0.000	0.003	0.001	0.000	0.000	0.001	0.000	0.001
S	0.280	0.279	0.285	0.283	0.282	0.283	0.280	0.274	0.281	0.282	0.282	0.281	0.280
Al	0.001	0.000	0.000	0.000	0.000	0.000	0.001	0.001	0.000	0.000	0.001	0.000	0.000
P	0.004	0.008	0.004	0.001	0.002	0.002	0.004	0.014	0.005	0.002	0.004	0.003	0.005
Fe : S	0.526	0.517	0.480	0.518	0.523	0.520	0.506	0.519	0.519	0.523	0.513	0.529	0.526
S : P	73.650	36.755	66.438	221.488	115.315	126.248	66.340	19.904	60.591	177.437	75.082	87.880	55.955

<b>Sample</b>	c3-3	c3-4	c4-1	c4-2	c4-3	c4-4	c5-1	c5-2	c5-3	c5-4	c5-5	c6-1	c6-2
<b>Atomic proportion</b>													
K	0.001	0.001	0.002	0.001	0.002	0.001	0.001	0.000	0.001	0.001	0.000	0.000	0.001
Ca	0.001	0.003	0.004	0.001	0.006	0.004	0.003	0.001	0.002	0.002	0.001	0.000	0.002
Fe	0.147	0.145	0.141	0.146	0.142	0.141	0.146	0.145	0.145	0.146	0.147	0.148	0.144
Na	0.004	0.008	0.010	0.004	0.012	0.008	0.004	0.002	0.003	0.003	0.002	0.002	0.005
Ba	0.000	0.000	0.000	0.000	0.000	0.000	0.000	0.000	0.000	0.000	0.000	0.000	0.000
Mn	0.000	0.000	0.000	0.000	0.000	0.000	0.000	0.000	0.000	0.000	0.000	0.000	0.000
Mg	0.000	0.001	0.005	0.001	0.005	0.003	0.000	0.001	0.002	0.000	0.000	0.000	0.001
Si	0.000	0.001	0.001	0.000	0.000	0.000	0.000	0.001	0.002	0.000	0.000	0.000	0.001
S	0.282	0.280	0.277	0.282	0.276	0.279	0.282	0.283	0.281	0.282	0.283	0.283	0.282
Al	0.000	0.000	0.000	0.000	0.000	0.000	0.000	0.000	0.000	0.000	0.000	0.000	0.000
P	0.003	0.006	0.011	0.004	0.011	0.009	0.003	0.001	0.003	0.003	0.002	0.001	0.004
Fe : S	0.521	0.518	0.510	0.519	0.512	0.504	0.519	0.511	0.516	0.518	0.520	0.522	0.513
S : P	105.862	45.633	25.263	73.359	24.136	31.134	91.147	220.754	104.829	102.224	185.948	239.567	77.460

<b>Sample</b> <b>Atomic proportion</b>	c6-3	c6-4	c6-5	c6-6	d1-1	d1-2	d1-3	d2-1	d2-2	d2-3	d2-4	d2-5	d3-1
K	0.001	0.000	0.000	0.000	0.001	0.001	0.001	0.001	0.005	0.000	0.001	0.001	0.003
Ca	0.001	0.001	0.001	0.000	0.003	0.002	0.004	0.001	0.003	0.001	0.001	0.001	0.004
Fe	0.143	0.143	0.146	0.147	0.136	0.138	0.137	0.148	0.154	0.146	0.154	0.146	0.143
Na	0.005	0.002	0.002	0.001	0.002	0.002	0.002	0.001	0.008	0.001	0.002	0.002	0.009
Ba	0.000	0.000	0.000	0.000	0.000	0.000	0.000	0.000	0.000	0.000	0.000	0.000	0.000
Mn	0.000	0.000	0.000	0.000	0.000	0.000	0.000	0.000	0.000	0.000	0.000	0.000	0.000
Mg	0.000	0.001	0.000	0.000	0.000	0.001	0.001	0.000	0.000	0.000	0.000	0.000	0.001
Si	0.007	0.001	0.002	0.001	0.000	0.001	0.001	0.000	0.002	0.000	0.001	0.001	0.000
S	0.278	0.283	0.282	0.283	0.285	0.284	0.283	0.282	0.272	0.283	0.280	0.283	0.278
Al	0.001	0.000	0.001	0.000	0.000	0.000	0.000	0.000	0.001	0.000	0.000	0.000	0.000
P	0.003	0.002	0.002	0.001	0.003	0.003	0.005	0.002	0.014	0.002	0.001	0.002	0.010
Fe : S	0.512	0.505	0.516	0.520	0.478	0.487	0.486	0.526	0.564	0.517	0.550	0.518	0.516
S : P	100.369	145.185	166.048	291.042	95.846	103.425	56.759	145.355	20.088	188.214	193.173	131.827	27.120

Sample Atomic proportion	d3-2	d3-3	d3-4	d4-1	d4-2	d4-3	d4-4	d4-5	e1-1	e1-2	e1-3	e1-4	e2-1
K	0.003	0.001	0.001	0.003	0.002	0.001	0.002	0.001	0.001	0.002	0.070	0.002	0.001
Ca	0.004	0.000	0.002	0.003	0.001	0.001	0.001	0.001	0.001	0.004	0.267	0.003	0.001
Fe	0.142	0.146	0.145	0.140	0.146	0.143	0.145	0.145	0.150	0.144	0.000	0.150	0.148
Na	0.009	0.002	0.005	0.009	0.005	0.004	0.004	0.003	0.004	0.008	0.205	0.009	0.004
Ba	0.000	0.000	0.000	0.000	0.000	0.000	0.000	0.000	0.000	0.000	0.001	0.000	0.000
Mn	0.000	0.000	0.000	0.000	0.000	0.000	0.000	0.000	0.000	0.000	0.001	0.000	0.000
Mg	0.001	0.000	0.001	0.002	0.001	0.001	0.001	0.001	0.000	0.002	0.070	0.001	0.001
Si	0.000	0.000	0.000	0.002	0.000	0.000	0.000	0.000	0.001	0.001	0.026	0.000	0.001
S	0.280	0.284	0.282	0.279	0.281	0.283	0.282	0.283	0.281	0.278	0.000	0.278	0.281
Al	0.000	0.000	0.000	0.000	0.000	0.000	0.000	0.000	0.000	0.000	0.016	0.000	0.000
P	0.009	0.001	0.005	0.009	0.005	0.004	0.004	0.003	0.003	0.009	0.422	0.007	0.003
Fe : S	0.507	0.513	0.515	0.503	0.517	0.507	0.513	0.514	0.536	0.519		0.539	0.527
S : P	31.294	215.769	57.850	31.797	61.580	79.402	68.643	110.272	88.993	31.476	0.000	38.889	95.563

<b>Sample</b> <b>Atomic proportion</b>	e2-2	e2-3	e2-4	e3-1	e3-2	e3-3	e3-4	e4-1	e4-2	e4-3	e4-4	e4-5	e5-1
K	0.001	0.002	0.001	0.002	0.001	0.001	0.000	0.003	0.001	0.001	0.001	0.001	0.001
Ca	0.002	0.006	0.002	0.006	0.001	0.001	0.001	0.002	0.002	0.001	0.001	0.001	0.001
Fe	0.146	0.144	0.148	0.144	0.147	0.149	0.145	0.143	0.147	0.149	0.148	0.146	0.148
Na	0.006	0.008	0.003	0.008	0.002	0.002	0.002	0.011	0.006	0.004	0.003	0.004	0.004
Ba	0.000	0.000	0.000	0.000	0.000	0.000	0.000	0.000	0.000	0.000	0.000	0.000	0.000
Mn	0.000	0.000	0.000	0.000	0.000	0.000	0.000	0.000	0.000	0.000	0.000	0.000	0.000
Mg	0.001	0.001	0.001	0.002	0.001	0.000	0.001	0.002	0.001	0.001	0.001	0.001	0.001
Si	0.002	0.000	0.000	0.000	0.000	0.000	0.000	0.001	0.000	0.000	0.000	0.000	0.000
S	0.280	0.279	0.281	0.277	0.282	0.282	0.283	0.279	0.281	0.282	0.281	0.282	0.281
Al	0.001	0.000	0.000	0.000	0.000	0.000	0.000	0.000	0.000	0.000	0.000	0.000	0.000
P	0.004	0.007	0.002	0.012	0.003	0.002	0.002	0.008	0.004	0.003	0.003	0.004	0.004
Fe : S	0.523	0.518	0.527	0.519	0.520	0.527	0.514	0.513	0.523	0.528	0.527	0.518	0.525
S : P	70.743	42.282	113.717	23.765	107.204	138.930	147.057	35.726	62.488	90.867	108.738	79.725	74.135

<b>Sample</b>	<b>e5-2</b>	<b>e5-3</b>	<b>e5-4</b>	<b>e5-5</b>
<b>Atomic proportion</b>				
K	0.001	0.000	0.007	0.001
Ca	0.001	0.000	0.003	0.001
Fe	0.145	0.149	0.110	0.147
Na	0.003	0.002	0.009	0.002
Ba	0.000	0.000	0.000	0.000
Mn	0.000	0.000	0.000	0.000
Mg	0.001	0.000	0.003	0.000
Si	0.001	0.000	0.003	0.000
S	0.282	0.283	0.287	0.283
Al	0.000	0.000	0.001	0.000
P	0.003	0.002	0.011	0.002
Fe : S	0.515	0.526	0.385	0.522
S : P	86.115	178.750	27.022	123.345

Sample	Average mass proportion (%)										
	K <sub>2</sub> O	CaO	FeO	Na <sub>2</sub> O	BaO	MnO	MgO	SiO <sub>2</sub>	SO <sub>3</sub>	Al <sub>2</sub> O <sub>3</sub>	P <sub>2</sub> O <sub>5</sub>
Non-coated	0.02	0.01	61.83	0.03	0.01	0.01	0.05	0.18	136.78	0.06	0.00
B (t 20)	0.56	1.19	58.90	0.53	0.02	0.02	0.45	0.79	127.49	0.18	2.52
C (t 20)	0.24	0.68	60.40	0.82	0.01	0.02	0.22	0.32	130.26	0.09	1.62
D (t 10)	0.40	0.60	58.91	0.71	0.00	0.03	0.14	0.20	127.94	0.07	1.86
E (t 10)	0.46	0.93	61.10	1.01	0.03	0.01	0.30	0.22	131.47	0.10	2.51

Sample	Average atomic proportion												
	K	Ca	Fe	Na	Ba	Mn	Mg	Si	S	Al	P	Fe : S	S : P
Non-coated	0.002	0.001	0.136	0.001	0.000	0.000	0.007	0.021	0.269	0.006	0.000	0.504	
B (t20)	0.019	0.032	0.120	0.016	0.000	0.000	0.018	0.025	0.234	0.006	0.052	0.514	59.240
C (t20)	0.001	0.002	0.145	0.005	0.000	0.000	0.001	0.001	0.281	0.000	0.004	0.517	112.452
D (t10)	0.002	0.002	0.144	0.004	0.000	0.000	0.001	0.001	0.281	0.000	0.005	0.514	95.201
E (t10)	0.005	0.014	0.139	0.014	0.000	0.000	0.004	0.002	0.268	0.001	0.024	0.517	80.251

## BIOGRAPHY

Mr. Nipon Kongmak was born on October 18, 1980 in Bangkok, capital city of Thailand. He had finished the primary school in 1992 from Assumption College Thonburi, Bangkok and graduated in the secondary school in 1998 from Taweethapisek School, Bangkok. After that, he entered Chulalongkorn University. He received the Bachelor of Science degree in Geology from Department of Geology, Faculty of Science, Chulalongkorn University in 2002. Then, he subsequently entered the Master's degree program by getting partial scholarship in Environmental and Hazardous Waste Management, Inter-Department of Environmental and Hazardous Waste Management, Chulalongkorn University.



สถาบันวิทยบริการ  
จุฬาลงกรณ์มหาวิทยาลัย